Title: Mechanistic model for design, analysis, operation and control of microalgae cultures: calibration and application to tubular photobioreactors

Corresponding Author: Professor Joan Garcia, PhD

Corresponding Author's Institution: Technical University of Catalonia

First Author: Alessandro Solimeno

Order of Authors: Alessandro Solimeno; Francisco G Acíen Fernández; Joan Garcia, PhD

Abstract: Closed photobioreactors (PBRs) are usually used for the production of high-value microalgae biomass at higher productivities than in open ponds. A large variety of different PBRs have been developed to optimize the biomass productivity and photosynthesis efficiency. At the same time mathematical models for PBRs are also increasing in popularity for design of new systems and for improving understanding of the complex processes occurring inside. The aim of the present study is to calibrate of the new mechanistic model for microalgae growth using experimental data from two different tubular photobioreactors. Hydrodynamic and light attenuation through the medium were added in the model to obtain a realistic representation of photobioreactor. Furthermore, the model was able to predict microalgae production under different climatic conditions and the oxygen accumulation throughout the photobioreactor.

GEMMA. GROUP OF ENVIRONMENTAL
ENGINEERING AND MICROBIOLOGY
UPC

Dear Editor,

We have received the comments from the Editor and Reviewers, and we have modified the manuscript accordingly. Comments suggested were considered, the manuscript and the captions of the figures have been carefully modified in order to meet the suggestions.

Furthermore, the manuscript has been edited by a native English speaking Lauren Parker from the California Polytechnic State University of San Luis Obispo.

We hope that the revised manuscript fully complies with comments and suggestions addressed by Reviewers.

Yours sincerely,

Joan García Serrano

Corresponding author

Answers to reviewer's comments

 (Comments in black and answers in red)

Reviewer #1:

Re reviewer has accepted the revisions, a few minor comments below. During my last read of the manuscript I noted a number of minor corrections and areas that need further clarification directly on the PDF of the document, which you can download from the EES system. Also, the manuscript should be edited by a native english speaking colleague. Please provide a final revision that appropriately addresses these suggestions for final approval.

Reviewer #1: Most of the proposed corrections were adequately addressed, I can recommend this MS for publication now.

Well done. Regards!

L315 extent   instead of extend

We have modified the manuscript accordingly. Comments suggested were considered, the manuscript and the captions of the figures have been carefully modified in order to meet the suggestions.

Furthermore, the manuscript has been edited by a native English speaking Lauren Parker from the California Polytechnic State University of San Luis Obispo.

1. Introduction

~~Microalgae biomass production is an industrial sector that continues growing each year. Products made from microalgae are nowadays presented by industry as a natural and green solution to the energy, food, economic and climate challenges facing the Earth [1, 20]. Although still there are some technical challenges (e.g. cost efficient production and harvesting systems), in general it is believed that microalgae fuels, feeds, plastics and other chemicals will be price competitive within the next years. Some are price competitive already [15, 31].~~

~~Another potential market application of microalgae is their use in the context of wastewater treatment. Although this is not a new application, the feasibility of microalgae cultures for wastewater treatment and at the same time encouraging resource recovery and feedstock production has revived the interest on this technology [13]. Microalgae treatment systems are currently viewed as a future alternative to conventional activated sludge treatment plants, where produced biomass can be valorised in the form of biofuels or bioproducts therefore optimising treatment costs [25, 29].~~

~~In practice, industrial~~ Industrial production of microalgae can be accomplished in open or closed photobioreactors. Open systems are ~~made up by~~ shallow channels in the shape of race track~~s~~ (raceway reactors) ~~which~~ and have been extensively studied in the past [9, 15]. Though open photobioreactors represent an efficient economic solution in front of closed photobioreactors, they ~~can be more~~ can be easily contaminated by ~~other~~ microorganisms ~~different from those of the culture,~~ and ~~are more~~ difficult to control. These disadvantages make closed photobioreactors more suitable when high-value products are the target of the culture. ~~These c~~ Closed systems ~~allow a strict~~ strictly control ~~of~~ chemical, physical and biological factors and can ~~better match ideal~~ improve conditions for microalgae growth by optimizing light absorption due to turbulent conditions in the culture [9, 11, ~~33~~ 30, ~~34~~ 31].

Closed photobioreactors (as well as open raceways) are sensitive to carbon limitations and pH variations that could limit photosynthesis and therefore biomass production [16]. ~~This is usually~~Carbon and pH limitations ~~can be~~can be corrected by supplying carbon dioxide (CO_2^-) in order to maintain high photosynthesis rates and pH

control. However the two most critical issues of closed photobioreactors are the risk of overheating and their potential for oxygen accumulation and subsequent growth inhibition [~~21~~20]. ~~Therefore~~To prevent overheating, closed photobioreactors often require cooling as well as degasser systems [~~35~~32]. Concentrations of dissolved oxygen (DO) in the culture above 250% ~~of~~air saturation ~~value~~can dangerously inhibit microalgae activity [12].

~~In the~~Over the last few decades, mathematical models have proven to be useful tools for the design, analysis, operation and control in multiple engineering problems [5]. Nowadays, models have become essential tools for understanding complex processes, such as those occurring in photobioreactors. In the case of microalgae cultures, models are ~~still in their infancy in comparison~~less developed than those seen in ~~to~~ other fields~~,~~. ~~and are not in common practice because most of them~~When models contain too ~~are based in~~ few parameters~~,~~. ~~and are not able to capture the~~they risk the capability ~~of not capturing the~~ complexity of microalgae cultures in long-~~-~~term scenarios, and therefore can be unreliable. Having this in mind, Solimeno et al. (2015) [~~29~~27] developed a ~~rather~~complete mechanistic mathematical model that includes crucial physical and biokinetic processes ~~for the~~that ~~description~~describe ~~of~~microalgae growth in different types of cultures, ~~and in~~particularly in wastewater (where growth is controlled by carbon and nitrogen limitations~~for growth can be significant~~). This model was calibrated with data from a complete stirred culture fed with simulated treated wastewater using a 0D domain [~~29~~27]. A global sensitivity analysis was carried out using the same ~~data set~~set of data [~~30~~28]. In the present paper we intend to go beyond our previous work~~s~~, calibrating the model with data from ~~more complex systems~~

consisting of two different pilot scale tubular closed photobioreactors fed with different types of medium culture. In this present case, a 2D domain, which is used to represents the hydrodynamics of the system (i.e., transport of diluted species and mass transfer phenomena), is coupled with the previous mechanistic model [2927]. The resulting model has been implemented into the COMSOL Multiphysics^{TM} software, which solves equations using the finite elements method (FEM).

The aim of the present study is therefore theto calibration calibrate of the new and more complex mechanistic model of Solimeno et al. (2015) [2927] using experimental data from two different tubular photobioreactors. Furthermore, tThe potential of the model is demonstrated by means of practical study cases in which we simulate oxygen concentrations (the most critical growth inhibition factor of closed photobioreactors) and predict microalgae production as a function of temperature and light intensity. Simulations show the potentiality of photobioreactor configurations to optimize microalgae production. The overall objective of this model is to become a reference to simulate physical, chemical and biokinetic microalgae processes in different types of photobioreactors fed with different types of medium cultures.

2. Methods

2.1 Pilot closed photobioreactors and experimental data

Both photobioreactors were located in Spain, one in "Estación Experimental Las Palmerillas", property of Fundación CAJAMAR in Almeria, and the other in "Agropolis", property of Universitat Politècnica de Catalunya-BarcelonaTech in Barcelona (Fig. 1). The vertical tubular photobioreactor (PBR) in Almeria includes a loop solar receiver made of transparent plastic tubes of 0.09 m diameter with a total horizontal length of 400 m, and a 0.4 m diameter bubble column with 3.5 m of height, and has a total working volume of 3,000 L. The PBR unit is used to produce the

microalgae *Scenedesmus almeriensis*, which is characterized by a high growth rate~~,~~ ~~supporting~~ and tolerance temperatures up to 45 °C and ~~tolerance to~~ pH values up to 10 [1, ~~27~~25]. The ~~culture~~ PBR works by creating continuou~~ssl~~y flow of ~~cultures~~ between ~~the~~ loop and bubble column by means of a centrifuge pump located at the bottom of the column. The pump provides a constant flow velocity of 0.8 m s^{-1} inside the loop. The pH of the culture is controlled by ~~on demand~~ injection of pure CO_2 at 5 L min^{-1}. In the bubble column, excess ~~dissolved oxygen~~DO ~~in excess~~ is removed by a constant airflow rate of 140 L min^{-1}. ~~Furthermore,T~~ the culture temperature is ~~controlled~~ maintained ~~through an internal heat exchanger located at the bubble column~~ by passing cooling water at 1500 L h^{-1} through an internal heat exchanger located inside the bubble column~~for cooling~~. When fresh culture medium is poured into the system, ~~The~~ the culture is harvest~~ed~~ ~~of the culture is reaped~~ through an overflow ~~at the~~located on top of the column.~~ when fresh culture medium is poured into the system~~. Temperature, pH and ~~dissolved oxygen~~DO are measured at several locations along the tube using Crison probes (Crison Instruments, Spain) connected to a control-transmitter unit MM44 (Crison Instrument, Spain~~);~~). ~~liquid~~ Liquid and gas flow rates are measured using digital flowmeters (PF2W540 and PF2A510, from SMC, Japan). All of these ~~measures~~ monitoring systems are in turn connected to a control computer through a data acquisition device NI Compact FieldPoint (National Instruments, USA) [15]. Data for the present study ~~were~~ were obtained at the end of ~~an~~ a two month experiment ~~of 2 months~~ in which the photobioreactor was operated in continuous mode~~,~~ ~~at a~~ medium flow rate of 1020 L d^{-1}, and under controlled pH (7.8) and temperature (lower than 35 °C). As a result, the amount of microalgae biomass ~~amount~~ was kept fairly constant. Culture medium used was Mann&Myers, prepared using agricultural fertilizers. ~~Data~~ Collected data ~~used were~~were retrieved in batch mode by switching off the feeding ~~only~~ for 24 hours (at the end of the ~~2~~two months). Dissolved oxygen and pH data were recorded every 30 minutes, while temperature and irradiance were measured every hour.

108   The horizontal tubular photobioreactor in Barcelona is composed of 2 open-air

109 tanks made of polypropylene ~~with a size of~~and is 1.8 x 1 x 0.4 m (L x W x H) in size.

110 These tanks include paddlewheels that provide enough head pressure to move the

111 culture through 12 (6 per each flow direction) transparent 0.125 m diameter

112 polyethylene tubes (each 50 m in length ~~each one~~). Culture flows from one tank to the

113 other at a constant velocity of 0.125 m s^{-1}. Tanks also allow release of exceeding

114 oxygen accumulated along tubes. The PBR has an effective volume of 8.5 m^3. Note that

115 in this PBR there is no CO_2 injection or pH control. Data used for the present work were

116 retrieved from a 3 day's batch experiment and measured in each tank. For this

117 experiment the PBR was filled with 8 m^3 of agricultural runoff from a nearby

118 agriculture canal which were inoculated with 0.5 m^3 of inoculum with microalgae from

119 a previous experiment (Table 1). The PBR contained different microalgae species

120 belonging to the genus *Pediastrum sp.*, *Chlorella sp.* and *Scenedesmus sp.*

121   The horizontal PBR has dissolved oxygen and pH online sensors in each tank

122 that record data every hour, and temperature and irradiance online sensors that record

123 data every 2-3 hours. Gathered data are stored ~~via~~ using a Programmable Logic

124 Controller (PLC) that is connected to a computer with ~~a~~ supervisory control and a data

125 management system (Green web manager 2.0). During the ~~3~~ three days of experiments,

126 offline samples were taken every ~~2-3~~two-three hours and analyzed in the laboratory for

127 nitrates and alkalinity. Analysis of nitrat~~The~~ ion ~~chromatographic~~ chromatograpy

128 ~~analysis of nitrates~~ was accomplished using a Thermo Finnigan chromatograph with a

129 metallic detector TCD (thermal conductivity detector). ~~Alcalinity~~Alkalinity was

130 analysed using conventional titrimetric procedures indicated in ~~the~~ Standard Methods

131 [3]. Note that bicarbonate was calculated ~~from~~ using alkalinity measurements, pH, and

132 equilibrium constants of carbon species (Eq. 1).

133

134                    $$Alkalinity = 50 * \left[\frac{S_{HCO3}}{12} + 2 * \frac{S_{CO3}}{12} + S_{OH} - S_{H} \right] \qquad (1)$$

2.2 Conceptual model

The new mechanistic model presented by Solimeno et al. (2015) [~~29~~27] considers crucial physical, chemical and biokinetic processes for the description of microalgae growth in different types of cultures, ~~and most~~ particularly in wastewaters. The main relevant feature of the model, respect to any previous model for microalgae production [4, 6, ~~24~~23], consists in the inclusion of a carbon limitation on the growth of microalgae, as well as a dynamic model for photosynthesis, photolimitation,~~ and~~ light attenuation~~,~~, and ~~the description of the effect of~~ photorespiration. In the model, microalgae grow with light, consume nutrients (i.e., carbon and nitrogen), and release oxygen (Fig. 2).

Note that other nutrients (e.g., phosphorus) and micronutrients are not considered to be limiting factors because are usually highly available in wastewaters (which is the type of culture ~~that~~ mainly addresses by the model) [19]. Dependency of microalgae growth on phosphorus could ~~be~~ easily be implemented in the model ~~through~~ by creating a limiting Monod function, similar how the other ~~like the other~~ nutrients (i.e., carbon and nitrogen) were represented. In the model, as a result of microalgal activity in the presence of light, hydroxide ions concentration and pH increase. ~~Such i~~Increases in pH displace the equilibrium of the carbon species towards the formation of carbonates (which are not bioavailable for growth). Note that this model assumes that carbon dioxide as well as bicarbonate are bioavailable for growth. In darkness, endogenous respiration of microalgae release carbon dioxide, the concentration of hydrogen ions increase and the pH decreases. ~~By~~ With decreasing pH, the carbon equilibrium shifts and carbonate turns into bicarbonate, which can be used as substrate again in the presence of light [~~33~~30]. A detailed description of the model, ~~their~~ includings components, and processes can be found in Solimeno et al. (2015) [~~29~~27]. A

161 list of the processes included in the model, the equations describing their rates and the

162 matrix of stoichiometric parameters are shown in Supplementary Tables (4-5).

163 *2.3 Model domain*

164 The Pphotobioreactor's configuration was assumed to have a 2D geometry. The

165 domain was divided into two sub-domains (D1 and D2) corresponding to the loop

166 configuration and the bubble column for the vertical system in Almeria, and to the

167 open-air tanks and the tubes for the horizontal system in Barcelona (Fig. 3). In the case

168 of the vertical system, D1 was 400 m long in the longitudinal direction and 0.09 m in

169 diameter, while in the horizontal system it was 50 m long and 0.125 m in diameter. D2

170 domains were designed allocating the volume of the bubble column (vertical system)

171 and open-air tank (horizontal system) along a surface interface area through

172 whichwhere gases can bewere transferred to the atmosphere, fixing the corresponding

173 D1 diameter. Thus, the bubble column is defined with 3.3 m length long and 0.09 m

174 widthdeep, while the tank is 5.76 m long and 0.125 m widthdeep. These simplifications

175 allow to to simulatesimulate ofthe hydrodynamics of within the systems. Note that in

176 the present model it was necessary to divide the domain into two sub-domains due to

177 the different domain conditions. Transfer of gases to the atmosphere takes took place

178 exclusively in the bubble column and open-air tanks. A periodic condition was applied

179 at boundaries 1 and 2 to reproduce the continuous culture flow from domain 2 to 1

180 (degasser to loop and tank to tube).

181 *2.4 Hydrodynamics of the system, light attenuation and temperature*

182 In our previous work [2927], the calibration of the model was conducted in a

183 complete mixed reactor represented by a 0D domain in order to simplify

184 hydrodynamic's complexity. In the present work, as a result of the motion of the culture

185 through the tubes and bubble column or open-air tank, a 2D domain was needed, which

including~~ing~~ hydraulic and transport equations. On the other hand, in the previous work [~~28~~26], it was assumed that microalgae cells captured photons at all depths (light attenuation was neglected due to 0D domain). ~~In the~~The present work incorporates light attenuation due to the presence of ~~is added, including light limitations related to scattering and mutual shading effects of~~ microalgae.

In the model microalgae processes are influenced by temperature [~~29~~27]. It is known that the growth rate of microalgae is highly dependent on ~~increases when~~ temperature; it increases when ~~goes up to an~~ optimum temperature is reached and ~~decrease~~ drastically decreases when ~~with~~ optimum temperature ~~over the opt~~is exceeded~~imum~~ [14]. In the present study, microalgae production was simulated in a study case at different temperatures, showing the dependence of microalgae growth on temperature.

Hydrodynamics of system was modelled through the COMSOL Multiphysics[TM] software, previously used for the calibration of the microalgae model in a ~~complete~~ completly stirred experiment, which solves differential equations using the finite elements method (FEM).

2.4.1 Hydraulic Considerations

In the PBR used in this work the culture is set in motion by an external pump (vertical system) or by paddlewheels (horizontal system), and enters the model domain with a certain velocity. To predict the flow regime without starting a simulation, the Reynolds number was firstly calculated. The Reynolds number quantifies the ratio of inertia to viscous forces, characterizing the flow regime (Eq. 2):

$$Re = \frac{\rho * v * d}{\mu} \tag{2}$$

where ρ is the culture density (~~it is~~ assumed to have the same density as water, 1000 kg m^{-3}), v is the culture velocity (m s^{-1}), d is the tube diameter (0.09 m and 0.125 m for

vertical and horizontal systems, respectively). and μ is the dynamic viscosity of the culture (assumed to be the same as water 0.003 kg m^{-1}s^{-1}). The Reynolds number was calculated to be approximately 27,000 for the vertical system and 5,000 for the horizontal. Note that in tubes with a flow with a Reynolds number above 4,000 is already considered turbulent [~~32~~29], and in these conditions transversal variations of culture properties (temperature, dissolved oxygen, biomass concentration, etc.) may be neglected and Navier-Stokes equations can be solved directly. ~~At these~~With such high Reynolds number's temperature does not significantly influence the motion, because viscous forces (μ) are very small when compared to ~~the~~ inertial forces (ν~~), -). and temperature does not influence significantly the motion~~.

For turbulent flow, Comsol Multiphysics^{TM} solves the Navier-Stokes as well as continuity equations. Turbulent effects are modeled using "Turbulent Mixing" interfaces for "Transport of Diluted Species" physics. In "Turbulent Mixing" models the additional mixing caused by turbulence is estimated by adding turbulent diffusivity to the molecular diffusivity considering:

$$D_T = v_T / Sc_T \qquad (3)$$

where, D_T is the turbulent diffusion, v_T is the turbulent kinematic viscosity at 20 ^{o}C (1.004E-06 m^2 s^{-1}) and Sc_T is the turbulent Schmidt number (0.7).

2.4.2 Transport of dissolved and particulate components

Transport of diluted and particulate components with a concentration S_i [g m^{-3}] by convection and diffusion is given by:

$$\frac{\delta S_i}{\delta t} + (-D_T \cdot S_i) + \mathbf{u} \cdot c_i = r_i \qquad (4)$$

$$r_i = \sum_j v_{j,i} * \rho_j \qquad (5)$$

where i= 1,2…*m* are the different components considered (Table 2), and j is the number

of processes shown in Supplementary Table (4); u [m s^{-1}] is the vector of velocity, r$_i$ [g

m^{-3}s^{-1}] is the reaction rate, ρ [g m^{-3}s^{-1}] is the process rate corresponding to the biokinetic

and chemical j processes described in Solimeno et al. (2015) [2927] and v$_{j,i}$ is the

stoichiometric coefficient. Mathematical expressions of the stoichiometric coefficient

and values of biokinetic, physical and chemical parameters are shown in Supplementary

Tables (6-9).

2.4.3 Light attenuation

In the present study light intensity decay was described using Lambert-Beer's

Law, which dictates that intensity decreases exponentially as it penetrates into a

perfectly homogeneous section of the culture with a short penetration pathway [2725],

as it is the case of both PBR. In this case light is attenuated by the presence of

microalgae inside the reactors. The average light intensity (I$_{av}$, [μmol m^{-2}s^{-1}]) at any

point within the culture is therefore calculated as [17]:

$$I_{av} = I_o \cdot \psi \, (1\text{-exp} \, (k_i \cdot X_{ALG} \cdot d) \, / \, k_i \cdot X_{ALG} \cdot d \qquad (6)$$

where, I$_o$ [μmol m^{-2}s^{-1}] is the incident light intensity, k$_i$ is the extinction coefficient for

microalgae biomass [0.1 m^2 g^{-1}] [8], X$_{ALG}$ is the concentration of microalgae, ψ ψ is the

solar irradiance fraction available in the reactor and d [m] is the diameter of tube.

2.4.4 Temperature

In our model, the influence of temperature on microalgae activity was

implemented by the thermic photosynthetic factor (f$_{T,FS}$), that which takes into account

the effects of temperature on microalgae growth, and also on endogenous respiration

and inactivation processes (1a, 1b, 2 and 3 in Supplementary Table 4, respectively).

259 Water temperature varies ~~on~~ both on hourly and daily scales, ~~affecting~~ affecting ~~both~~

260 microalgal photosynthesis and respiration rates. The thermic photosynthetic factor is

261 represented in the model following the work of Dauta et al. (1990) [14]:

$$f_{T,FS}(T) = e^{-\left(\frac{T-T_{opt}}{s}\right)^2} \tag{7}$$

263 where T_{opt} (optimum temperature) was assumed ~~equal~~ to be 25 °C [14] and s equal to 13

264 [14] (it is a parameter value for empirical fitting).

2.5 Calibration procedure

266 Model output~~s~~ results are ~~very~~ highly ~~sensitivity~~ sensitive to the maximum

267 specific growth rate of microalgae (μ_{ALG}), ~~and the~~ mass transfer coefficient for oxygen

268 ($K_{a,O2}$), and carbon dioxide ($K_{a,CO2}$). ~~Especially the~~The mass transfer coefficients

269 depend on the extension of the surface interface and photobioreactor design [~~29~~27].

270 Therefore, these parameters were calibrated in the two different tubular

271 photobioreactors. The model was first calibrated using experimental data obtained from

272 the vertical photobioreactor located in Almeria (Spain). Dissolved oxygen, pH,

273 temperature and irradiance were monitored for 24 hours on ~~28th of~~ February 28th, 2012.

274 Afterwards, the model was calibrated with experimental data from the horizontal

275 photobioreactor located in Barcelona (Spain). Data used for this calibration were

276 retrieved from ~~a 3~~three day~~s's~~ batch experiment from April 16th, 2012 to April 19th,

277 2012. ~~of April.~~ Available data used for the calibration procedure are shown in

278 Supplementary Tables (1-2). The initial concentrations of components in the vertical

279 and horizontal photobioreactors at the beginning of the experiments are shown in Table

280 3. In the horizontal PBR the concentrations of NH_4^+ and NH_3 were lower than the

281 analytical method`s detection limit ~~of the analytical method~~ and therefore ~~are~~

282 considered to be zero for ~~the~~ this model ~~as 0~~. Note ~~that~~ the difference in initial

283 concentrations of microalgae (X_{ALG}) ~~is different in~~between the two PBRs due to their

284 different operating conditions

2.6 Study cases

286   Practical study cases have been done to evaluate the influence of both

287 temperature and irradiance on microalgae production, and the effect of oxygen

288 concentration in the loop. The vertical photobioreactor of Almeria (Spain) was selected

289 as reference for these studies.

290   Starting from the initial concentrations used for ~~the~~ calibration of the model in

291 the vertical photobioreactor, average daily microalgae production was simulated using

292 daily temperature and irradiance variations ~~of~~ from ~~the~~ 17th day of each month of year.

293 Two scenarios were evaluated. In the first set of simulations the vertical photobioreactor

294 was under controlled temperature by passing cooling water at 1500 L/h through an

295 internal heat exchanger located in the bubble column of the photobioreactor. In a second

296 set of simulations, temperature was obtained from meteorological annals of Almeria

297 (Spain). ~~An estimation of the total annual production for these~~ These two scenarios

298 were compared and an estimation of the total annual production using monthly

299 irradiance variations was calculated. Irradiance, expressed as photosynthetically active

300 radiation (PAR), was estimated for Almeria (Spain) from the mathematical equations

301 presented in Supplementary Table 10 [2].

302   Moreover, ~~keeping the reactor under controlled temperature,~~ oxygen

303 concentration throughout the 400 m ~~length~~ of ~~the~~ vertical photobioreactor was evaluated

304 while maintaining the reactor under controlled temperature,~~.~~ Dissolved oxygen profile

305 in the loop configuration was simulated at noon in the months of July and January,

306 when ~~it was recorded~~ the highest and lowest temperature, respectively, were recorded.

307 ~~and irradiance, respectively.~~

308

3. Results

In this work simulations for two different photobioreactors were studied. First we present the results of the model calibration for the vertical photobioreactor. Fig. 4 shows that the model was able to accurately match ~~dissolved oxygen~~DO and pH trends over the course of one day inside the system, with decreasing ~~and how~~ pH ~~decreases during the day~~ due to CO_2 injection (which displaces the equilibrium of carbon species). ~~As can be seen the model is able to accurately capture pH variations.~~

Fig. 5 shows the results of the calibration in the horizontal photobioreactor. Experimental and simulated dissolved oxygen and pH values inside the open-air tanks of the horizontal photobioreactor are presented. As can be seen, the wavelike trend of pH varied ~~with a general wavelike trend~~ due to microalgae activity, which is quite well simulated by the model. Moreover, Fig. 6 shows the experimental and simulated nitrate (N_NO$_3$) and bicarbonate (C_HCO$_3$) concentrations in the horizontal system. The model was able to reproduce quite well the trend of experimental data. In absence of ammonia species, only nitrates are used as nitrogen substrates for microalgae growth. The low concentration of nitrate in the culture medium limited the activity of microalgae. As can be seen, microalgae consumed ~~quickly~~ nitrate concentrations quickly in the first hours of experiment (Fig. 6). Likewise, Fig. 6 shows that bicarbonate concentrations decreased faster in the first hours due to intense microalgae activity. After 22 hours, in absence of nitrate, daily variations of bicarbonate are related to changes in equilibrium species of carbon.

Note that, in general, simulations of the vertical PBR were more accurate than those of the horizontal due to ~~the fact that in~~ in the horizontal system there was some growth of other microorganisms different from microalgae (e.g., bacteria and protozoa~~);~~). This was to be expected as the culture water ~~for culture~~ was from an irrigation channel. The activity of these microorganisms ~~affected~~ affected simulated factors

335 | though~~t~~ it is not known to ~~which~~ what ~~extend~~extent, because unfortunately we ~~haven't~~

336 | ~~numbers~~do not have values for ~~this~~ these organisms.

337 | Table 4 presents the values of the parameters that were calibrated in each

338 | photobioreactor. Note that maximum specific growth rate (μ_{ALG}) and the transfer of

339 | gases to the atmosphere ($K_{a,O2}$ and $K_{a,CO2}$) were also calibrated in our previous works

340 | [~~29~~27, ~~30~~28]. In this previous work~~s~~ the -model output results are ~~demonstrated to be~~

341 | very sensitive to these parameters [~~29~~27, ~~30~~28], and therefore should be calibrated with

342 | great accuracy. Furthermore, ~~especially~~ gas transfer parameters depend on the extension

343 | of the surface interface. Due to different PBRs design~~ of the PBR~~, modifications of

344 | these parameters were considered worthwhile.

345 |

346 | **4. Discussion**

347 | *4.1 New features of the model*

348 | In comparison to our previous work [~~29~~27], where a 0D domain was applied,

349 | here ~~in the present work a~~ 2D domain was used to represent the two tubular

350 | photobioreactors. The domain was divided in two sub-domains (D1 and D2), where

351 | different conditions from the tubes (D1) to the open body (D2) of the photobioreactors

352 | were applied. According to the function of bubble column in the vertical system and the

353 | open-air tank in the horizontal system, the transfer of gases to the atmosphere was only

354 | applied to the D2 domain that ~~corresponded~~ corresponds to the total volume of these

355 | specific parts.

356 | A periodic condition was applied at boundaries 1 and 2 to reproduce the

357 | recirculation of flow from the loop configuration to the bubble column in the vertical

358 | system, and from the tubes to the open-tank in the horizontal system. Simulation results

359 | demonstrated that these simplifications were adequate to describe the specific parts of

360 | different tubular photobioreactors. Moreover, fluid flow and transport equations were

361 added in the current model to obtain a realistic representation of the hydrodynamic~~s~~ in

362 the photobioreactors.

363 ~~Respect from~~In addition to the previous~~ly~~ mechanistic model presented by

364 Solimeno et al. (2015) [~~29~~27] light attenuation through the medium was implemented.

365 Light intensity decays exponentially due to microalgae biomass ~~accumulated~~

366 accumulation inside the reactors. Assuming a perfect mixing of medium, due to

367 turbulent flow regime, an irradiance average I_{av} was used to represent any point ~~of~~

368 ~~the~~within the reactor.

369

370 *4.2 Calibration of the model*

371

372 Results of the sensitivity analysis, reported in our previous work [~~30~~28], had

373 indicated that the maximum specific growth rate of microalgae (μ_{ALG}) and the mass

374 transfer coefficient for oxygen ($K_{a,O2}$) and carbon dioxide ($K_{a,CO2}$) were the parameters

375 with the greatest impact on simulation outputs. Therefore, calibration of these

376 parameters ~~have to be calibrated~~must be occur in each particular case.

377 The calibrated maximum specific growth rate of microalgae (μ_{ALG} = 1.7 [d^{-1}]) in

378 the vertical photobioreactor fits well within literature range [0.4-2.0 d^{-1}]. Also, the mass

379 transfer coefficient in the bubble column for oxygen which was $K_{a,O2}$ = 2.9E-03 s^{-1} fits

380 into the range values for vertical photobioreactors [1.2E-03 to 7.7E-03 s^{-1}] [18]. The

381 mass transfer coefficient for carbon dioxide ($K_{a,CO2}$= 2.8E-03 s^{-1}) was consistent with

382 range values [1.1E-03-7.0E-03 s^{-1}] for bubble column systems [18]. These same

383 parameters were calibrated with experimental data over ~~3~~three days from the horizontal

384 photobioreactor located in Barcelona (Spain). Likewise ~~the previously~~as in the previous

385 calibration, the values generated for the maximum growth rate of microalgae (μ_{ALG} =

386 1.7 [d^{-1}])~~and,~~ the mass transfer of oxygen ($K_{a,O2}$ = 9.2E-03 [s^{-1}]) and carbon dioxide

$(K_{a,CO_2} = 9.0\text{E-}03 \ [s^{-1}])$ were all in agreement with literature ranges for tubular photobioreactors [9].

Mass transfer coefficients depend on ~~the~~, temperature, ~~the~~ mixing and ~~especially~~ most importantly, the extension of the surface interface. Thus, variable values of mass transfer coefficients from vertical and horizontal photobioreactors are due to different design and scale-up of bubble column and open-tanks, respectively.

Also the culture medium influences the mass transfer coefficients and the maximum growth rate of microalgae. In this work the horizontal photobioreactor was filled with agricultural runoff ~~in~~ which could be ~~present~~ cointein few concentrations of bacteria and other microorganisms. The activity of these microorganisms could influence dissolved oxygen and carbon dioxide concentrations in the medium culture, and therefore could slightly affect the values of the calibrated parameters. However, single microscopic observations during the experiment indicated that their concentration was irrelevant in comparison to microalgae (as usual in this type of PBR), and thus their influence is considered very low or almost negligible. Calibrating the model in two different photobioreactors (e.g.~~,~~ horizontal and vertical) ~~and using~~with different types of media has ~~allowed to determinate~~proved the robustness and resilience of the mathematical model to operate under variables conditions. ~~of the mathematical model, which can operate under variables conditions.~~

4.3 Study case: microalgae production as a function of temperature and irradiance

Irradiance and temperature play an important role in microalgae production. These physical factors influence biokinetic and chemical processes related to microalgae growth. Irradiance is strictly correlated to photosynthesis rate. At high level of irradiance, microalgae become 'light saturated' because photosynthesis cannot process more photons. As result, the rate of photosynthesis ~~starts to~~ progressively starts

414 to stabilize [9, 13]. Temperature influences the equilibrium of chemical species (carbon

415 and nitrogen), ~~the~~ uptake of nutrients, ~~and~~ transfer of gases to the atmosphere, ~~but~~ and

416 especially the microalgae growth rates. The optimal temperature for microalgae growth

417 ranges between 15ºC and 25ºC, depending on the species [5, 19]. Temperature above or

418 below this range negatively affects ~~negatively~~ biomass yield~~s~~.

419   Thanks to the model, previously calibrated with daily experimental data, has

420 been possible to make predictions of microalgae production over long- term ~~knowing~~

421 with different environmental factors, such as temperature and irradiance. Simulations of

422 the average daily microalgae production at a monthly scale in the vertical

423 photobioreactor are presented in Fig 7. As can be observed simulations indicate that

424 production is generally higher under daily temperature variations due to a more

425 favo~~u~~rable temperature range (Supplementary Table 3). Table 5 presents the annual

426 microalgae production comparing the two scenarios studied: under controlled

427 temperature and with daily temperature variations. Although the growth of microalgae

428 decreases ~~by~~ with high temperature and irradiance during the months of June, July and

429 August (when the highest temperatures of the year occur), total annual production of

430 microalgae exposed to daily temperature variations is higher than the reactor under

431 controlled temperature. To optimize production, it might be considered to only use

432 cooling water ~~might be only used~~ during the hottest months (June, July and August).

433 Moreover, simulations results show that during the summer the production is also

434 inhibited due to high dissolved oxygen concentrations throughout~~thorought~~ loop

435 configuration up to 250% of air saturation (see next section).

436

437
438 *4.4 Study case: oxygen concentration*

439

440   Fig. 8 shows the simulations of the dissolved oxygen profile throughout the 400

441 m length of the vertical photobioreactor at noon (when the highest temperature occurs)

in the months of January and July. These two months were selected as they represent the minimum and maximum microalgae activity in a monthly basis time scale. As can be seen, the lower light intensity and temperature in January gives as a result lower dissolved oxygen concentrations in contrast to July. Also it can be observed in both months how dissolved oxygen concentration increases throughout the loop and decreases in the bubble column. In July, transfer of excess of dissolved oxygen to the atmosphere throughout the airlift permits to re-establish, at the beginning of loop configuration, the oxygen level under the maximum concentration of oxygen dissolved in water (32 gO_2 m^{-3}) equal 350% of saturation (9.07 gO_2 m^{-3}) [1, 8]. This property of the photobioreactor design is especially important in warm months (such as July), when a high photosynthetic activity could cause inhibition due to oxygen accumulation.

The model presented in this work allows to simulate and study microalgae growth inhibition due to high dissolved oxygen concentrations thanks to the inclusion of a photorespiration factor $f_{PR}(S_{O2})$ [~~29~~27]. The function ($f_{PR}(S_{O2})$) in Fig. 9 describes that for dissolved oxygen concentrations lower than the 250% S_{O2}^{SAT} (22.67 gO_2 m^{-3}) the photosynthesis rate is reduced ~~of~~ by 10%. Above this value, the photosynthesis rate decrease more quickly with a vertical asymptote and is equal at zero when dissolved oxygen reaches the 350% saturation limit (τS_{O2}^{SAT}= 32 gO_2 m^{-3}).

In process design, the current model can be used to ~~study which could be~~find the maximum photobioreactor length to avoid oxygen inhibition. ~~Here, as~~For example, ~~we present~~ for the month of July, simulations were conducted using half the previous~~in which we analyse what is the effect of reducing the~~ bubble column volume ~~to the half~~ (from 0.44 m^3 to 0.22 m^3) in the vertical photobioreactors loops ~~of~~ (400 m and 250 m). As seen in Fig. 10, ~~shows simulation results, and as can be seen~~ reducing the volume of the bubble column and ~~keeping~~ keeping the original loop configuration length (400 m), the simulation results show that the DO ~~dissolved oxygen~~ exceeds the saturation limit ~~and wil~~l inhibit~~ing~~ microalgae growth. The volume of bubble column is not enough to

469 transfer the excess of dissolved oxygen to the atmosphere. On the contrary, simulations

470 indicate that a 250 m length, photobioreactor greatly reduces the oxygen accumulation.

471

472 **5. Conclusion**

473

474   In this paper ~~the~~ a new mechanistic model to simulate microalgae growth was

475 calibrated in two different tubular photobioreactors. Fluid flow, transport equations and

476 light attenuation were included in the model described in our previous work and

477 implemented in COMSOL Multiphysics[TM] software. ~~Uncertainly~~ Uncertainty

478 parameters from previous~~ly~~ ~~sensibility~~ sensitivity analysis were calibrated in each

479 ~~particular~~ photobioreactor. The results of calibration indicate that the mass transfer of

480 gases and the maximum specific growth rate of microalgae fit well within literature

481 ranges. Moreover, the developed model demonstrates potential prediction of oxygen

482 accumulation throughout the loop configuration and daily microalgae production as a

483 function of temperature and irradiance. The model proves to be an efficient tool for

484 photobioreactor design and production ~~production~~ optimization.~~.~~

485

486 **References**

487 [1] Acién Fernández F.G., Fernández Sevilla, J.M., Molina Grima, E.   2013.

488 Photobioreactors for the production of microalgae. Reviews in Environmental Science

489 and Bio/Technology, Volume 12, Issue 2, pp 131-151.

490 [2] Al-Rawahi, N.Z., Zurigat, Y.H., Al-Azri N.A. 2011. Prediction of Hourly Solar

491 Radiation on Horizontal and Inclined Surfaces for Muscat/Oma. The Journal of

492 Engineering Research, Vol 8, No 2, 19-31.

493

494 [3] APHA-AWWA-WPCF, 2001. APHA-AWWA-WPCF Standard Methods for the

495 Examination of Water and Wastewater, twentieth ed. American Public Health

496 association, Washington DC.

497

498 [4] Bernard, O., Masci, P., Sciandra, A., 2009. A photobioreactor model in nitrogen

499 limited conditions. In: Proceedings of the sixth conference on mathematical model- ling,

500 Vienna.

501 [5] Bitog, J.P., Lee, I.-B., Lee, C.-G., Kim, K.-S., Hwang, H.-S., Hong, S.-W., Seo, I.-

502 H., Kwon, K.-S., Mostafa, E. 2011. Application of computational fluid dynamics for

503 modelling and designing photobioreactors for microalgae production: A review.

504 Computers and Electronics in Agriculture, 76(2), 131–147.

505 [6]. Bonachela, J.A., Raghib, M., Levin, S.A. 2011. Dynamic model of flexibile

506 phytoplankton nutrient uptake. Proc. Natl. Acad. Sci. U.S.A. 108, 20633-200638.

507 [7] Boussiba, S. Shadler, T., Karamanos, T.Y., Mollion, J., Morva, H., Verdus, M.C.,

508 Christiaen, D. 1986 Anabaena azollae as a nitrogen biofertilizer. Algal biotechnology,

509 169-178.

510 [8] Camacho Rubio F., García Camacho F., Fernández Sevilla J.M., Chisti Y., Molina

511 Grima E., 2003. A mechanistic model of photosynthesis in microalgae. Biotechnol

512 Bioeng. 81(4): 459–73.

513 [9] Camacho Rubio F., Acién Fernández F.G., García Camacho F., Sánchez Pérez J.A.,

514 Molina Grima E., 1999. Prediction of dissolved oxygen and carbon dioxide

515 concentration profiles in tubular photo- bioreactors for microalgal culture.

516 Biotechnology and bioengineering 62, 71–86.

517   [10] Carvalho, L. B., Souza, M. C., Bianco, M. S., Bianco, S. 2011. Estimativa da área

518   foliar de plantas daninhas de ambiente aquático: Pistia stratiotes. Planta daninha, v. 29,

519   n. 1, p. 65-68, 2011.

520   [11] Chisti, Y., 2007. Biodiesel from microalgae. Biotechnology Advances 25, 294-

521   306.

522   [12] Costache T. A, Acién Fernández F.G., Morales M., Fernández Sevilla J.M.,

523   Stamatin, I., Molina, E., 2013 Comprehensive model of microalgae photosynthesis rate.

524   Appl Microbiol Biotechnol., 17:7627-37

525   [13] Craggs, R.J., Heubeck, S., Lundquist, T.J., Benemann, J.R. 2011. Algae biofuel

526   from wastewater treatment high rate algal ponds. Water Sci. Technol. 63(4), 660-665.

527   [14] Dauta, A., Devaux, J., Piquemal, F., Boumnich, L. 1990. Growth rate of four

528   freshwater algae in relation to light and temperatura. Hydrobiologia 207, 221-226.

529   [15] Fernández, I. Acién, F.G., Berenguel, M., Guzmán J.L., Andrade, G.A., Pagano,

530   D.J. 2014. A Lumped parameter chemical-physical model for tubular photobioreactors.

531   Chemical Engineering Science 112, 116-129.

532   [16] Fernández, I., Acién, F.G., Fernández, J.M., Guzmán, J.L., Magán, J.J., Berenguel,

533   M. 2012. Dynamic model of microalgal production in tubular photobioreactor.

534   Biosource Technology 126, 172-181.

535   [17] Hase, R., Oikawa, H., Sasao, C., Morita, M., Watanabe, Y., 2000. Photosynthetic

536   production of microalgal biomass in a raceway system under greenhouse conditions in

537   Sendai city. J. Biosci. Bioeng. 89 (2), 157–163.

538   [18] Hulatt, C.J., Thomas, D.N., 2011. Productivity, carbon dioxide uptake and net

539   energy return of microalgal bubble column photobioreactors. Biosour. Technol. 102,

540   5775-5787.

541 [19] Larsdotter, K., 2006. Wastewater treatment with microalgae-a literature review. Vatten, 31–38.

543 ~~[20] Mata, T.M., Martins, A.A., Caetano, N.S., 2010. Microalgae for biodiesel production and other applications: a review. Renev. Sustain. Energy Rev. 14, 217-232.~~

545 [~~21~~20] Molina Grima, E., Fernández, J., Acién Fernández, G., Chisti, Y., 2001. Tubular photobioreactor design for algae cultures. Journal of biotechnology 92, 113–131.

547 [~~22~~21] Molina Grima, E., 1999. Mass culture methods. In: Flickinger, M.C., Drew, S.W. (Eds.), Encyclopedia of Bioprocess Technology: Fermentation, Biocatalysis and Bioseparation, vol. 3. Wiley, pp. 1753–1769.

550 [~~23~~22] Novak, J.T., Brune, D.E. 1985. Inorganic carbon limited growth kinetics of some freshwater algae. Water Res. 19, 215-225.

552 [~~24~~23] Packer A, Li Y, Andersen T, Hu Q, Kuang Y, Sommerfeld M. 2011. Growth and neutral lipid synthesis in green microalgae: a mathematical model. Bioresour Technol; 102:111–7.

555 ~~[25] Park, J.B.K., Craggs, R.J., Shilton, A.N., 2011a. Wastewater treatment high rate algal ponds for biofuel production. Bioresource Technology, 102(1), 35–42.~~

557 [~~26~~24] Reichert, P., Borchardt, D., Henze, M., Rauch, W., Shanahan, P., Somlyódy, L., Vanrolleghem, P., 2001. River Water Quality Model no. 1 (RWQM1): II. Biochemical process equations. Water science and technology : a journal of the International Association on Water Pollution Research 43(5), 11–30.

561 [~~27~~25] Sanchez, J.F., Fernández-Sevilla, J.M., Acíen, F.G., Ceron, M.C., Perez-Parra, J. & Molina-Grima, E., 2008. Biomass and lutein productivity of Scenedesmus almeriensis: influence of irradiance, dilution rate and temperature. Appl. Microbiol. Biotechnol., 79, 719–729.

[2826] Silva, H.J., Pirt, J. 1984. Carbon dioxide inhibition of photosynthetic growth of chlorella. Journal of General Microbiology, 130, 2833-2838.

[2927] Solimeno, A., Samsó, R., Uggetti, E., Sialve, B., Steyer, J.P., Gabarró, A., García, J. 2015. New mechanistic model to simulate microalgae growth. Algal Research 12, 350-358.

[3028] Solimeno. A., Samsó, R., García, J. 2016. Parameter sensitivity analysis of a mechanistic model to simulate microalgae growth. Algal Research 15, 217-223.

[31] Spolaore, P., Joannis-Cassan, C., Duran, E., Isambert, A. 2006. Commercial Applications of Microalgae. Journal of bioscience and bioengineering, 101, 87–96.

[3229] Stokes, G. 1851. On the Effect of the Internal Friction of Fluids on the Motion of Pendulums. Transactions of the Cambridge Philosophical Society 9: 8–106.

[3330] Ugwu, C.U., H. Aoyagi and H. Uchiyama, 2008. Photobioreactors for mass cultivation of algae. Bioresour. Technol., 99: 4021-4028.

[3431] Wang, B., Lan, Q., Horsman, M., 2012. Closed photobioreactors for production of microalgal biomasses. Biotechnology Advances 30 904–912.

[3532] Weissmand, J.C., Goebel, R.P., 1987. Design and Analysis of Microalgal Open Pond Systems for the Purpose of Producing Fuels. SERI/STR-231-2840.

[3633] Wu, X., Merchuk, J., 2001. A model integrating fluid dynamics in photosynthesis and photoinhibition processes. Chemical Engineering Science 56, 3527–3538.

Table 1. Agricultural runoff characteristics during batch experiment in the tubular

horizontal photobioreactor located in Barcelona (Spain).

Parameter	Agricultural runoff
pH	8.4
Dissolved oxygen (g m^{-3})	6.6
NO_3^--N (g m^{-3})	0.6
Alkalinity (g $CaCO_3$ m^{-3})	223

Table 2. Dissolved and particulate components considered in the model.

Component	Description	Units
Dissolved Components		
S_{NH4}	Ammonium nitrogen	gN-NH$_4$ m^{-3}
S_{NH3}	Ammonia nitrogen	gN-NH$_3$ m^{-3}
S_{NO3}	Nitrate nitrogen	gN-NO$_3$ m^{-3}
S_{CO2}	Carbon dioxide	gC-CO$_2$ m^{-3}
S_{HCO3}	Bicarbonate	gC-HCO$_3$ m^{-3}
S_{CO3}	Carbonate	gC-CO$_3$ m^{-3}
S_{O2}	Dissolved oxygen	gO$_2$ m^{-3}
S_H	Hydrogen ions	gH m^{-3}
S_{OH}	Hydroxide ions	gH-OH m^{-3}
Particulate Component		
X_{ALG}	Microalgae biomass	gTSS m^{-3}

Table 3. Initial concentrations of the components in the vertical photobioreactor of

Almeria (Spain) and horizontal photobioreactor of Barcelona (Spain).

Components	Concentrations		Units
	Vertical PBR	Horizontal PBR	
X_{ALG}	774.14	251	gTSS m^{-3}
S_{NH4}	14	-	gN-NH$_4$ m^{-3}
S_{NH3}	0.684	-	gN-NH$_3$ m^{-3}
S_{NO3}	4.2	0.6	gN-NO$_3$ m^{-3}
S_{CO2}	1.59	0.068	gC-CO$_2$ m^{-3}
S_{HCO3}	100	7.59	gC-HCO$_3$ m^{-3}
S_{CO3}	0.62	0.085	gC-CO$_3$ m^{-3}
S_{O2}	7.2	6.64	gO$_2$ m^{-3}
S_H	6.31E-6	3.55E-6	gH m^{-3}

S_{OH}	1.58E-3	2.82E-3	gH-OH m^{-3}

Table 4. Values of calibrated parameters in the vertical and horizontal photobioreactors.

Parameter	Description	Value	
		Vertical PBR	Horizontal PBR
μ_{ALG}	Maximum specific growth rate of microalgae	1.7 d^{-1}	1.7 d^{-1}
$K_{a,O2}$	Mass transfer coefficient for oxygen	2.9E-03 s^{-1}	9.2E-03 s^{-1}
$K_{a,CO2}$	Mass transfer coefficient for carbon dioxide	2.8E-03 s^{-1}	9.0E-03 s^{-1}

Table 5. Comparing total annual production under controlled temperature and daily

temperature variations versus optimizing system using cooling water during summer.

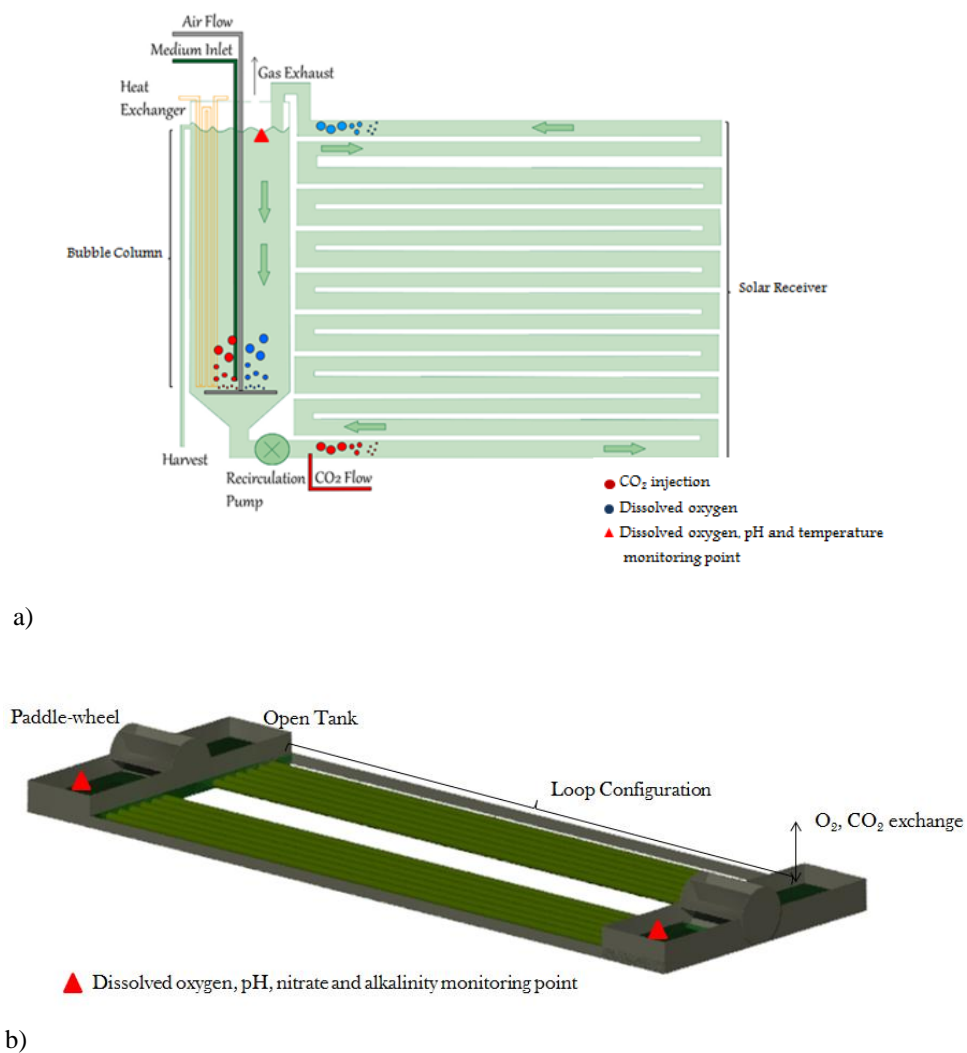| Total annual production	Value
Optimizing system	1796.86 gTSS m^{-3}
Daily temperature variations	1714.53 gTSS m^{-3}
Under controlled temperature	1604.48 gTSS m^{-3}

Figure

a)

b)

Fig. 1. a) Tubular vertical photobioreactor located in Almeria (Spain) with details of the solar receiver (a continuous tubular loop) and a mixing unit (a bubble column). The culture is continuously recirculating from one to the other part using airlift and mechanical pumps. [16], b) Tubular horizontal photobioreactor located in Barcelona (Spain) with details of the two open-air tanks and the loop configurations (6 tubes per each flow direction). Mechanical paddlewheels promote the recirculation of the culture through the system.
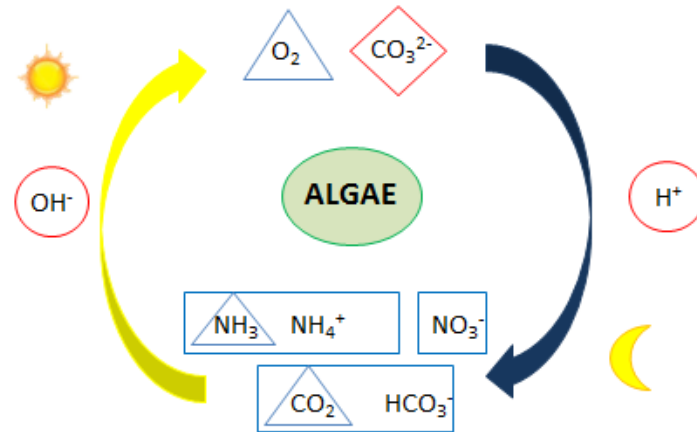
Fig. 2. General schematic representation of the conceptual model by Solimeno et al. (2015) [27]. Microalgae (green ellipse), substrates (rectangles), gaseous species (triangles) and species depending on algal activity which are neither substrates nor gases (diamonds and circles). Other nutrients (e.g. phosphorus) and micronutrients are not limiting factors.
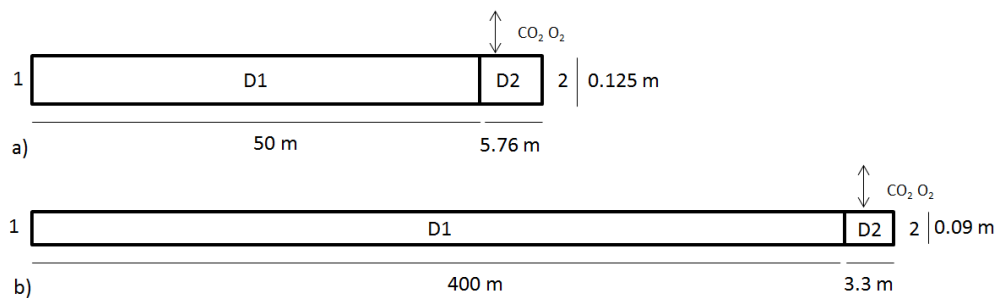

Fig. 3. Schematic representation of the model domain, a) simplification of the horizontal photobioreactor located in Barcelona (Spain), b) simplification of the vertical photobioreactor in Almeria (Spain). D1 represents the loop configuration of both PBRs and D2 is the the total volume of open-air tank (a) and bubble column (b) respectively for horizontal and vertical photobioreactor. A periodic condition was applied at boundaries 1 and 2 to reproduce the continuous culture flow.
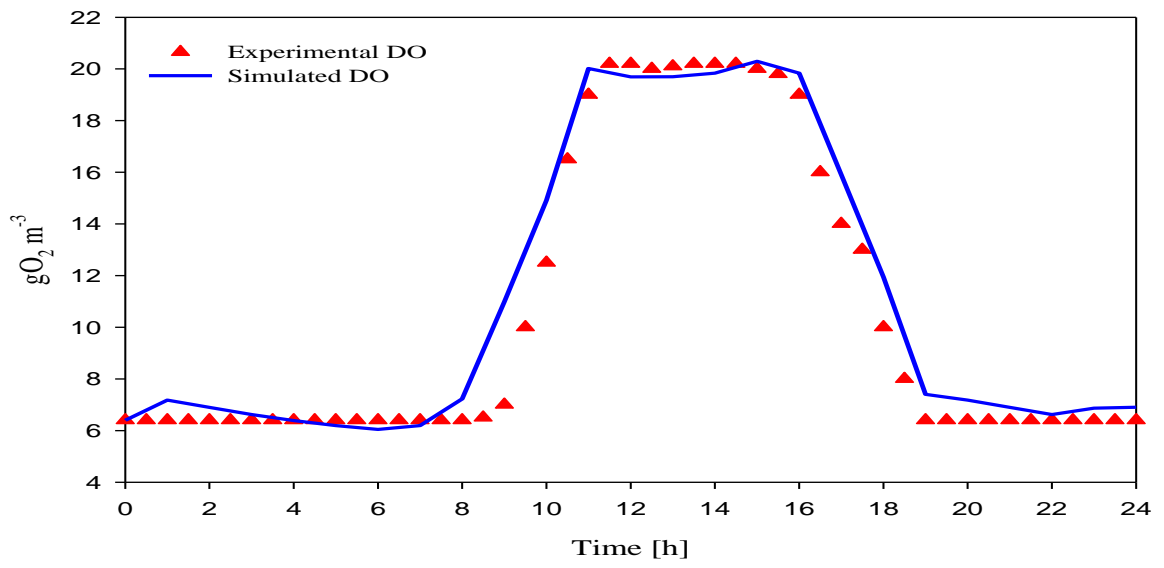
a)
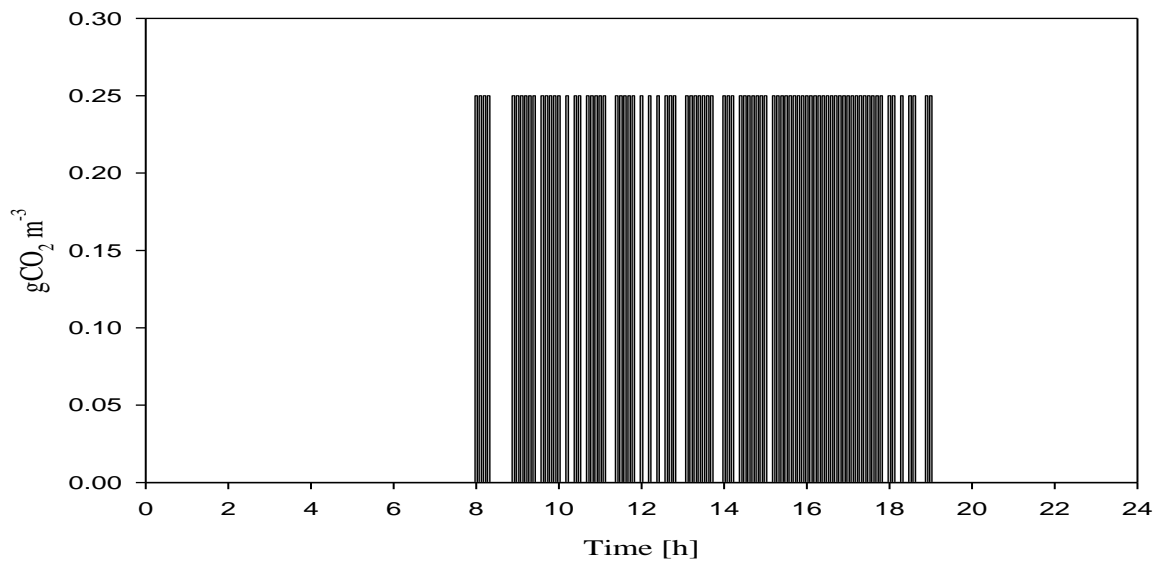
b)
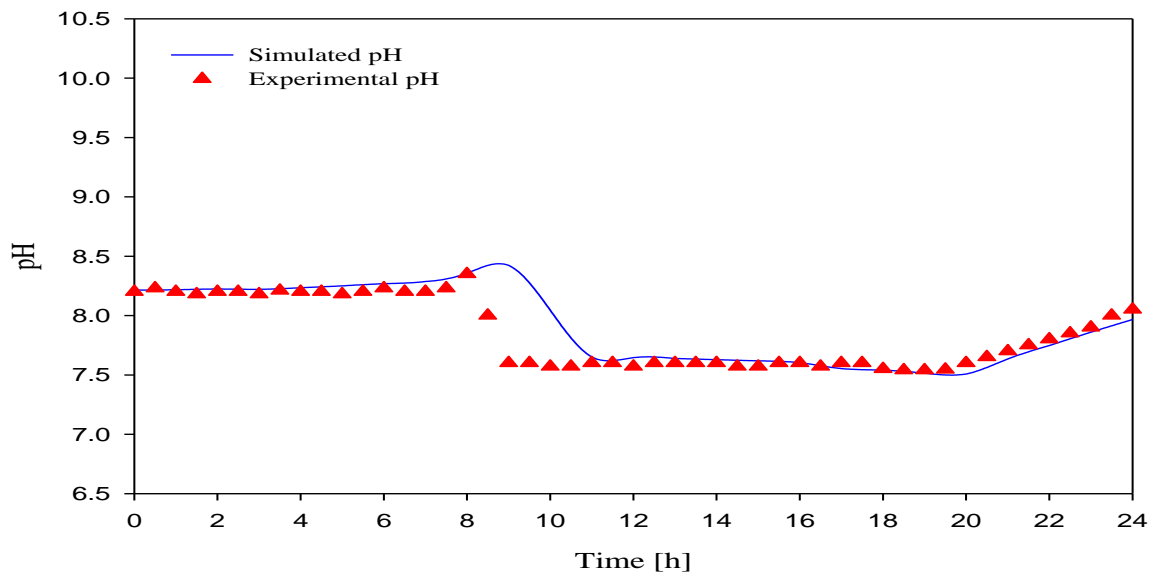
c)

Fig. 4. Experimental (red triangles) and simulated (blue line) (a) dissolved oxygen (DO) and (c) pH values as a function of CO_2 injection (b) over the 24 hours in the vertical photobioreactor in Almeria (Spain).
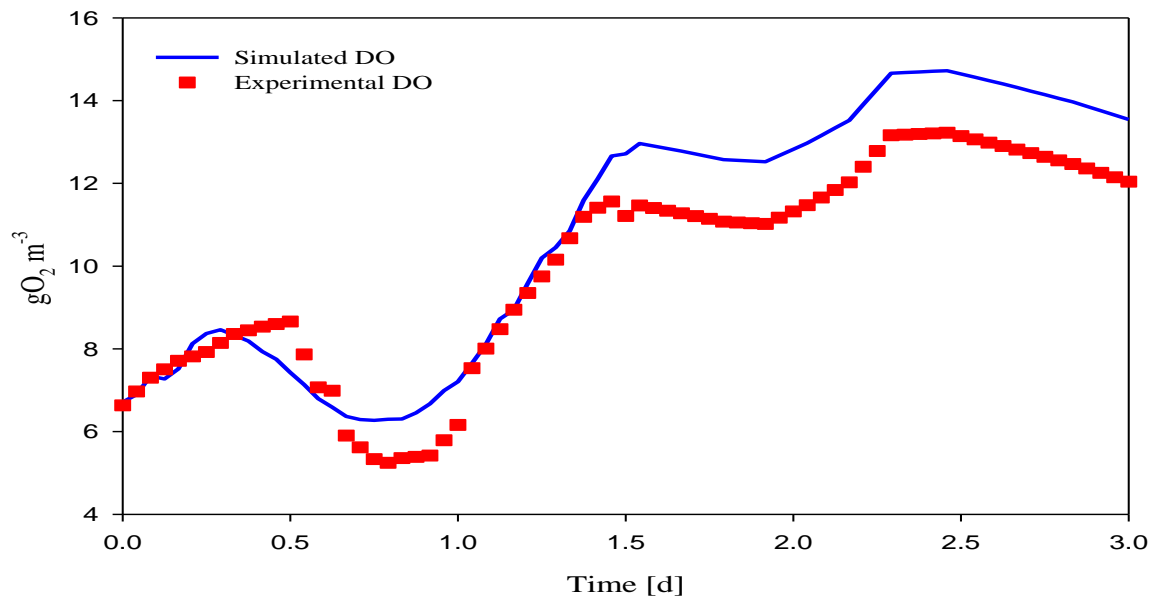
a)
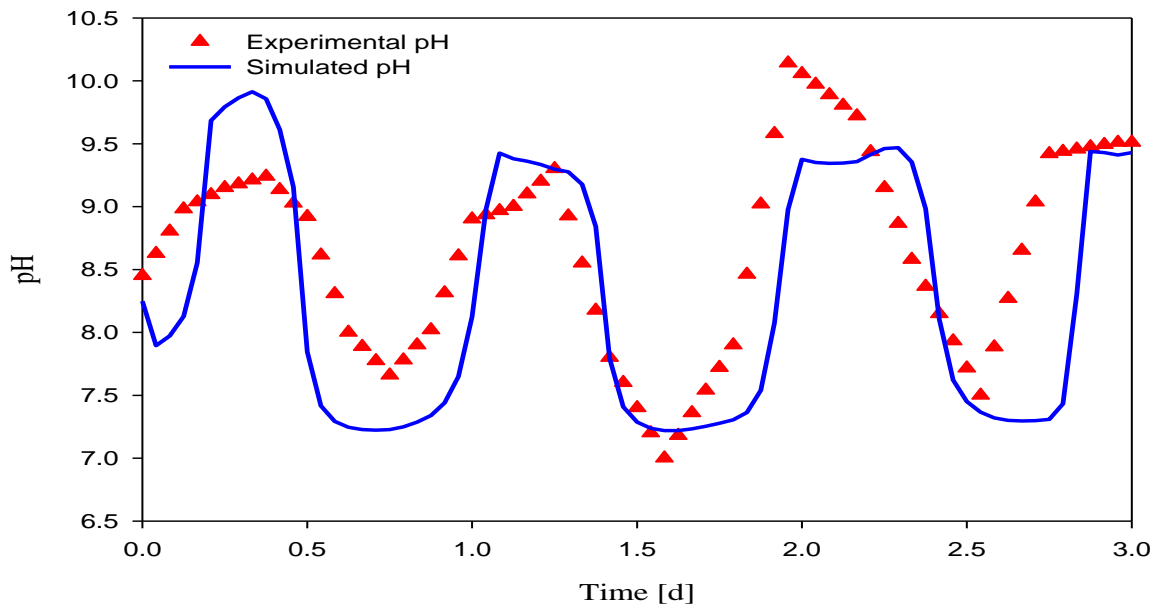
b)

Fig. 5. Experimental (red triangles) and simulated (blue line) (a) dissolved oxygen (DO) and (b) pH values over the three days in the horizontal photobioreactor in Barcelona (Spain).
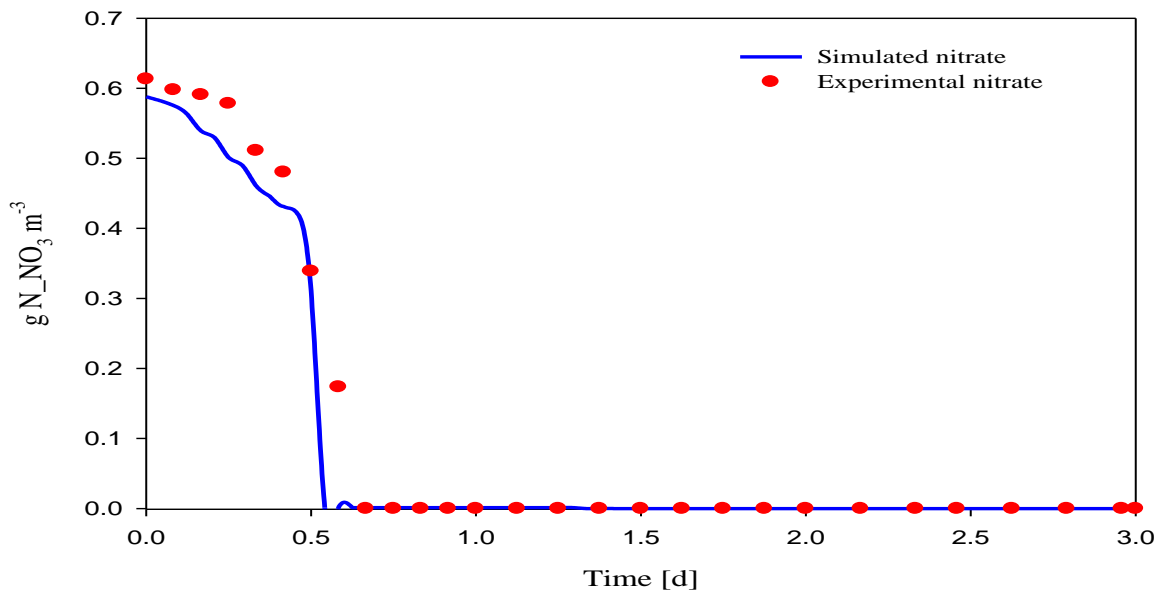
a)
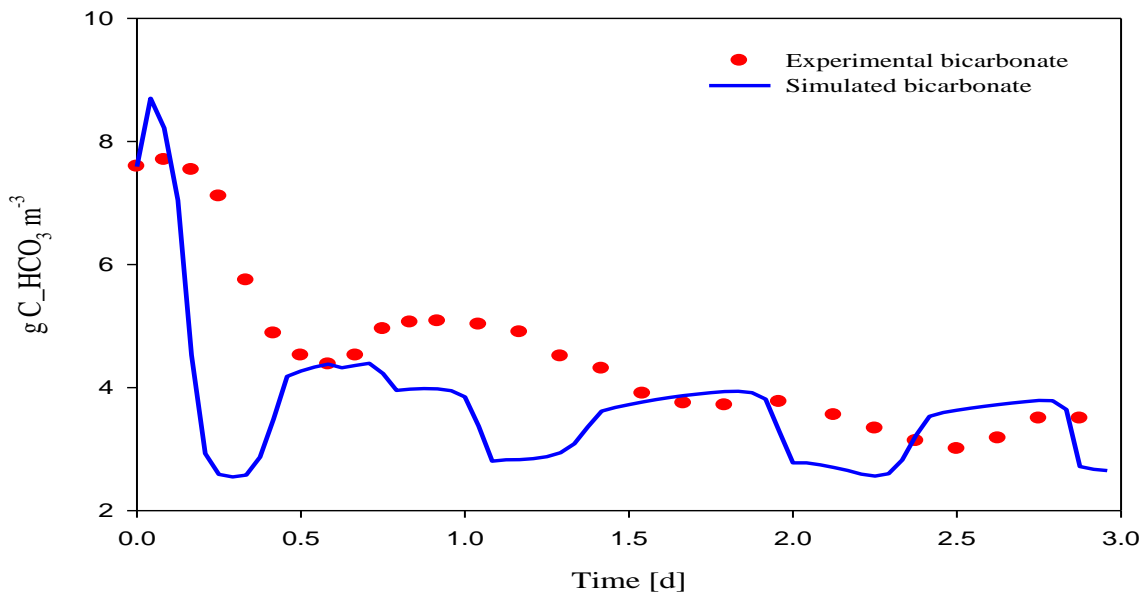
b)

Fig. 6. Experimental (red dots) and simulated (blue line) (a) nitrate and (b) bicarbonate concentrations over the three days in the horizontal photobioreactor in Barcelona (Spain).
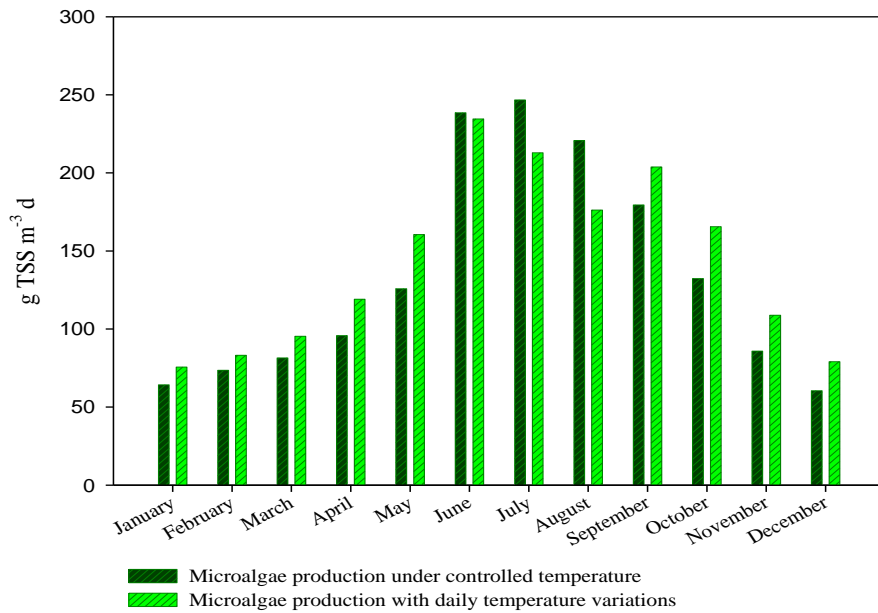
Fig. 7. Average daily microalgae production for each month of the year under controlled temperature and with daily temperature variations.
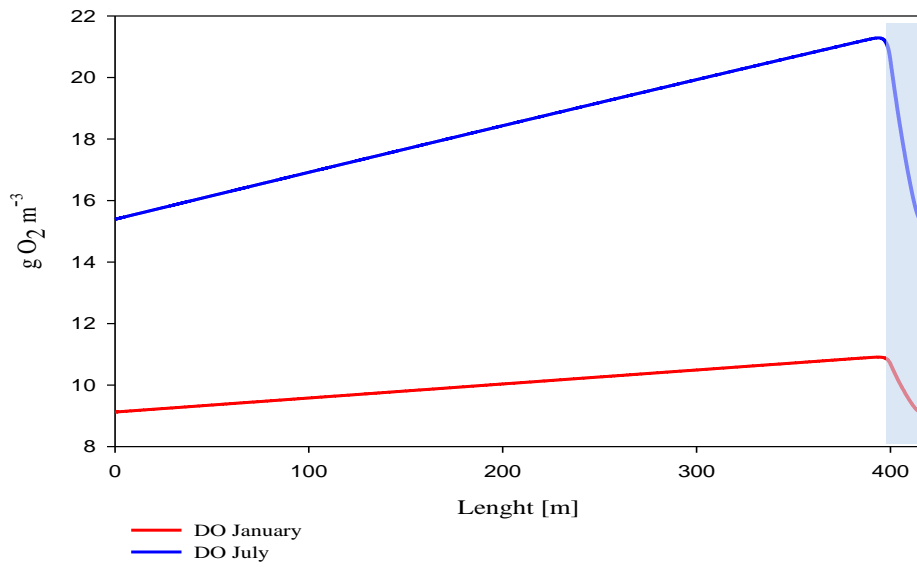
Fig. 8. Simulations of dissolved oxygen (DO) concentration profile throughout the vertical photobioreactor in Almeria (Spain) in the months of January and July. Bubble column position is represented by blue region.
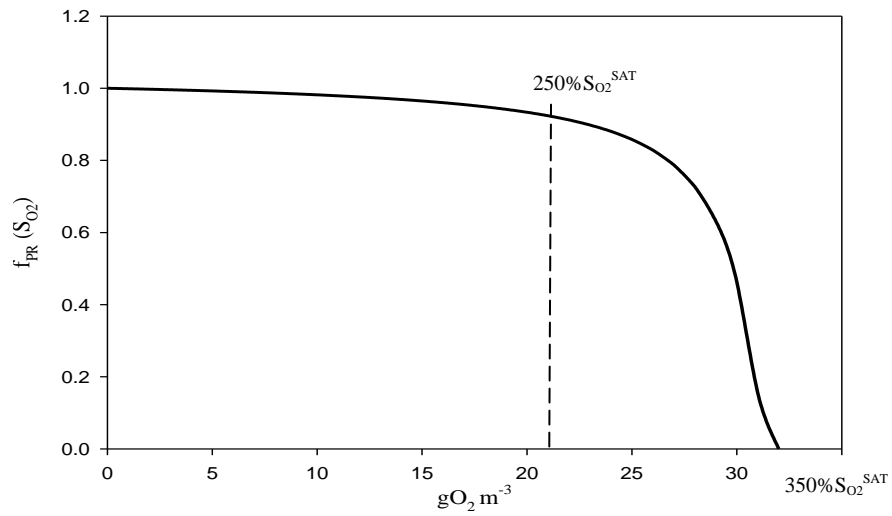
Fig. 9. Profile of photorespiration factor function for value of dissolved oxygen concentrations below the saturation limit (τS_{O2}^{SAT}).
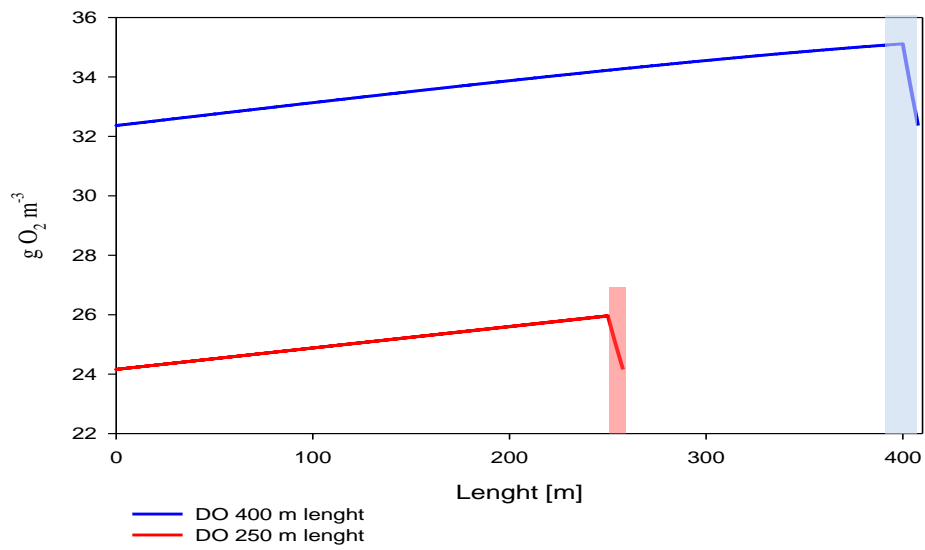
Fig. 10. Simulations of dissolved oxygen (DO) concentration profile throughout 400 m and 250 m length of the vertical photobioreactor in Almeria (Spain) in the months of July. Bubble column position is represented by blue and red rectangle, for 400 m and 250 m length of vertical photobioreactor, respectively.

Supplementary Material

Graphical abstract
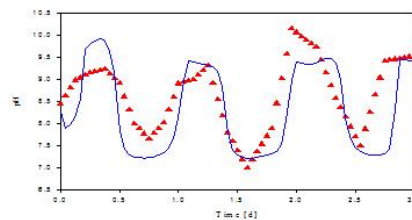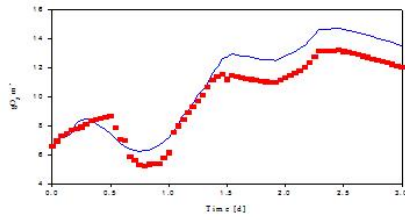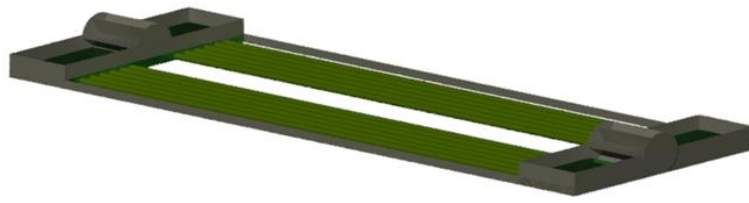
Highlights

- New mechanistic model for microalgae production in closed photobioreactors is developed.

- The model integrates the biological and engineering aspects of the systems.

- The accuracy of the model has been validated using real pH and dissolved oxygen values.

- The model has been verified in two different closed photobioreactors.

1. Introduction

Industrial production of microalgae can be accomplished in open or closed photobioreactors. Open systems are shallow channels in the shape of race tracks (raceway reactors) and have been extensively studied in the past [9, 15]. Though open photobioreactors represent an efficient economic solution in front of closed photobioreactors, they can be easily contaminated by microorganisms and difficult to control. These disadvantages make closed photobioreactors more suitable when high-value products are the target of the culture. Closed systems strictly control chemical, physical and biological factors and can improve conditions for microalgae growth by optimizing light absorption due to turbulent conditions in the culture [9, 11, 30, 31].

Closed photobioreactors (as well as open raceways) are sensitive to carbon limitations and pH variations that could limit photosynthesis and therefore biomass production [16]. Carbon and pH limitations can be corrected by supplying carbon dioxide (CO_2^-) in order to maintain high photosynthesis rates and pH control. However the two most critical issues of closed photobioreactors are the risk of overheating and their potential for oxygen accumulation and subsequent growth inhibition [20]. To prevent overheating, closed photobioreactors often require cooling as well as degasser systems [32]. Concentrations of dissolved oxygen (DO) in the culture above 250% air saturation can dangerously inhibit microalgae activity [12].

Over the last few decades, mathematical models have proven to be useful tools for the design, analysis, operation and control in multiple engineering problems [5]. Nowadays, models have become essential tools for understanding complex processes, such as those occurring in photobioreactors. In the case of microalgae cultures, models are less developed than those seen in other fields. When models contain too few parameters, they risk the capability of not capturing the complexity of microalgae cultures in long-term scenarios, and therefore can be unreliable. Having this in mind, Solimeno et al. (2015) [27] developed a complete mechanistic mathematical model that

28   includes crucial physical and biokinetic processes that describe microalgae growth in

29   different types of cultures, particularly in wastewater (where growth is controlled by

30   carbon and nitrogen limitations). This model was calibrated with data from a complete

31   stirred culture fed with simulated treated wastewater using a 0D domain [27]. A global

32   sensitivity analysis was carried out using the same set of data [28]. In the present paper

33   we intend to go beyond our previous work, calibrating the model with data from two

34   different pilot scale tubular closed photobioreactors fed with different types of medium

35   culture. In this present case, a 2D domain, which represents the hydrodynamics of the

36   system (i.e., transport of diluted species and mass transfer phenomena), is coupled with

37   the previous mechanistic model [27]. The resulting model has been implemented into

38   the COMSOL Multiphysics^{TM} software, which solves equations using the finite

39   elements method (FEM).

40   The aim of the present study is to calibrate the new and more complex

41   mechanistic model of Solimeno et al. (2015) [27] using experimental data from two

42   different tubular photobioreactors. The potential of the model is demonstrated by means

43   of practical study cases in which we simulate oxygen concentrations (the most critical

44   growth inhibition factor of closed photobioreactors) and predict microalgae production

45   as a function of temperature and light intensity. Simulations show the potential of

46   photobioreactor configurations to optimize microalgae production. The overall objective

47   of this model is to become a reference to simulate physical, chemical and biokinetic

48   microalgae processes in different types of photobioreactors fed with different types of

49   medium cultures.

50

51   **2. Methods**

52   *2.1 Pilot closed photobioreactors and experimental data*

53 Both photobioreactors were located in Spain, one in "Estación Experimental Las

54 Palmerillas", property of Fundación CAJAMAR in Almeria, and the other in

55 "Agropolis", property of Universitat Politècnica de Catalunya-BarcelonaTech in

56 Barcelona (Fig. 1). The vertical tubular photobioreactor (PBR) in Almeria includes a

57 loop solar receiver made of transparent plastic tubes of 0.09 m diameter with a total

58 horizontal length of 400 m, and a 0.4 m diameter bubble column with 3.5 m of height,

59 and has a total working volume of 3,000 L. The PBR unit is used to produce the

60 microalgae *Scenedesmus almeriensis*, which is characterized by a high growth rate and

61 tolerance temperatures up to 45 °C and pH values up to 10 [1, 25]. The PBR works by

62 creating continuous flow of culture between loop and bubble column by means of a

63 centrifuge pump located at the bottom of the column. The pump provides a constant

64 flow velocity of 0.8 m s^{-1} inside the loop. The pH of the culture is controlled by

65 injection of pure CO_2 at 5 L min^{-1}. In the bubble column, excess DO is removed by a

66 constant airflow rate of 140 L min^{-1}. The culture temperature is maintained by passing

67 cooling water at 1,500 L h^{-1} through an internal heat exchanger located inside the

68 bubble column. When fresh culture medium is poured into the system, the culture is

69 harvested through an overflow located on top of the column. Temperature, pH and DO

70 are measured at several locations along the tube using Crison probes (Crison

71 Instruments, Spain) connected to a control-transmitter unit MM44 (Crison Instrument,

72 Spain). Liquid and gas flow rates are measured using digital flowmeters (PF2W540 and

73 PF2A510, from SMC, Japan). All of these monitoring systems are in turn connected to a

74 control computer through a data acquisition device NI Compact FieldPoint (National

75 Instruments, USA) [15]. Data for the present study were obtained at the end of a two

76 month experiment in which the photobioreactor was operated in continuous mode,

77 medium flow rate of 1,020 L d^{-1}, and under controlled pH (7.8) and temperature (lower

78 than 35 °C). As a result, the amount of microalgae biomass was kept fairly constant.

79 Culture medium used was Mann&Myers, prepared using agricultural fertilizers.

80 Collected data were retrieved in batch mode by switching off the feeding for 24 hours

81 (at the end of the two months). Dissolved oxygen and pH data were recorded every 30

82 minutes, while temperature and irradiance were measured every hour.

83   The horizontal tubular photobioreactor in Barcelona is composed of two open-

84 air tanks made of polypropylene and is 1.8 x 1 x 0.4 m (L x W x H) in size. These tanks

85 include paddlewheels that provide enough head pressure to move the culture through 12

86 (6 per each flow direction) transparent 0.125 m diameter polyethylene tubes (each 50 m

87 length). Culture flows from one tank to the other at a constant velocity of 0.125 m s^{-1}.

88 Tanks also allow release of exceeding oxygen accumulated along tubes. The PBR has

89 an effective volume of 8.5 m^3. Note that in this PBR there is no CO_2 injection or pH

90 control. Data used for the present work were retrieved from a three days batch

91 experiment and measured in each tank. For this experiment the PBR was filled with 8

92 m^3 of agricultural runoff from a nearby agriculture canal which were inoculated with 0.5

93 m^3 of inoculum with microalgae from a previous experiment (Table 1). The PBR

94 contained different microalgae species belonging to the genus *Pediastrum sp.*, *Chlorella*

95 *sp.* and *Scenedesmus sp.*

96   The horizontal PBR has dissolved oxygen and pH online sensors in each tank

97 that record data every hour, and temperature and irradiance online sensors that record

98 data every two to three3 hours. Gathered data are stored using a Programmable Logic

99 Controller (PLC) that is connected to a computer with supervisory control and a data

100 management system (Green web manager 2.0). During the three days of experiments,

101 offline samples were taken every two-three hours and analyzed in the laboratory for

102 nitrates and alkalinity. Analysis of nitrate ion chromatography was accomplished using

103 a Thermo Finnigan chromatograph with a metallic detector TCD (thermal conductivity

104 detector). Alkalinity was analysed using conventional titrimetric procedures indicated in

105 Standard Methods [3]. Note that bicarbonate was calculated using alkalinity

106 measurements, pH, and equilibrium constants of carbon species (Eq. 1).

107

$$Alkalinity = 50 * \left[\frac{S_{HCO3}}{12} + 2 * \frac{S_{CO3}}{12} + S_{OH} - S_H \right] \qquad (1)$$

109

110   *2.2 Conceptual model*

111   The new mechanistic model presented by Solimeno et al. (2015) [27] considers

112   crucial physical, chemical and biokinetic processes for the description of microalgae

113   growth in different types of cultures, particularly in wastewaters. The main relevant

114   feature of the model, respect to any previous model for microalgae production [4, 6, 23],

115   consists in the inclusion of a carbon limitation on the growth of microalgae, as well as a

116   dynamic model for photosynthesis, photolimitation, light attenuation, and

117   photorespiration. In the model, microalgae grow with light, consume nutrients (i.e.,

118   carbon and nitrogen), and release oxygen (Fig. 2).

119   Note that other nutrients (e.g., phosphorus) and micronutrients are not

120   considered to be limiting factors because are usually highly available in wastewaters

121   (which is the type of culture mainly addresses by the model) [19]. Dependency of

122   microalgae growth on phosphorus could easily be implemented in the model by creating

123   a limiting Monod function, similar how the other nutrients (i.e., carbon and nitrogen)

124   were represented. In the model, as a result of microalgal activity in the presence of light,

125   hydroxide ions concentration and pH increase. Increases in pH displace the equilibrium

126   of the carbon species towards the formation of carbonates (which are not bioavailable

127   for growth). Note that this model assumes that carbon dioxide as well as bicarbonate are

128   bioavailable for growth. In darkness, endogenous respiration of microalgae release

129   carbon dioxide, the concentration of hydrogen ions increase and the pH decreases. With

130   decreasing pH, the carbon equilibrium shifts and carbonate turns into bicarbonate,

131   which can be used as substrate again in the presence of light [30]. A detailed description

132   of the model, including components, and processes can be found in Solimeno et al.

133   (2015) [27]. A list of the processes included in the model, the equations describing their

134   rates and the matrix of stoichiometric parameters are shown in Supplementary Tables

135   (4-5).

136   *2.3 Model domain*

137   The photobioreactor's configuration was assumed to have a 2D geometry. The

138   domain was divided into two sub-domains (D1 and D2) corresponding to the loop

139   configuration and the bubble column for the vertical system in Almeria, and to the

140   open-air tanks and the tubes for the horizontal system in Barcelona (Fig. 3). In the case

141   of the vertical system, D1 was 400 m long in the longitudinal direction and 0.09 m in

142   diameter, while in the horizontal system it was 50 m long and 0.125 m in diameter. D2

143   domains were designed allocating the volume of the bubble column (vertical system)

144   and open-air tank (horizontal system) along a surface interface area where gases were

145   transferred to the atmosphere, fixing the corresponding D1 diameter. Thus, the bubble

146   column is 3.3 m long and 0.09 m deep, while the tank is 5.76 m long and 0.125 m deep.

147   These simplifications allow to simulate of hydrodynamics within the system. Note that

148   in the present model it was necessary to divide the domain into two sub-domains due to

149   the different domain conditions. Transfer of gases to the atmosphere took place

150   exclusively in the bubble column and open-air tanks. A periodic condition was applied

151   at boundaries 1 and 2 to reproduce the continuous culture flow from domain 2 to 1

152   (degasser to loop and tank to tube).

153   *2.4 Hydrodynamics of the system, light attenuation and temperature*

154   In our previous work [27], the calibration of the model was conducted in a

155   complete mixed reactor represented by a 0D domain in order to simplify

156   hydrodynamic's complexity. In the present work, as a result of the motion of the culture

157   through the tubes and bubble column or open-air tank, a 2D domain was needed, which

158   include hydraulic and transport equations. On the other hand, in the previous work [26],

159   it was assumed that microalgae cells captured photons at all depths (light attenuation

160   was neglected due to 0D domain). The present work incorporates light attenuation due

161   to the presence of microalgae.

162   In the model microalgae processes are influenced by temperature [27]. It is

163   known that the growth rate of microalgae is highly dependent on temperature; it

164   increases when optimum temperature is reached and drastically decreases when

165   optimum temperature is exceeded [14]. In the present study, microalgae production was

166   simulated in a study case at different temperatures, showing the dependence of

167   microalgae growth on temperature.

168   Hydrodynamics of system was modelled through the COMSOL Multiphysics^{TM}

169   software, previously used for the calibration of the microalgae model in a completely

170   stirred experiment, which solves differential equations using the finite elements method

171   (FEM).

172   *2.4.1 Hydraulic Considerations*

173   In the PBR used in this work the culture is set in motion by an external pump

174   (vertical system) or by paddlewheels (horizontal system), and enters the model domain

175   with a certain velocity. To predict the flow regime without starting a simulation, the

176   Reynolds number was firstly calculated. The Reynolds number quantifies the ratio of

177   inertia to viscous forces, characterizing the flow regime (Eq. 2):

178    $$Re = \frac{\rho * v * d}{\mu} \qquad (2)$$

179   where ρ is the culture density (assumed to have the same density as water, 1000 kg m^{-3}),

180   v is the culture velocity (m s^{-1}), d is the tube diameter (0.09 m and 0.125 m for vertical

181   and horizontal systems, respectively), and μ is the dynamic viscosity of the culture

182   (assumed to be the same as water 0.003 kg m^{-1}s^{-1}). The Reynolds number was

183   calculated to be approximately 27,000 for the vertical system and 5,000 for the

184   horizontal. Note that in tubes with a flow with a Reynolds number above 4,000 is

185   already considered turbulent [29], and in these conditions transversal variations of

186   culture properties (temperature, dissolved oxygen, biomass concentration, etc.) may be

187   neglected and Navier-Stokes equations can be solved directly. With such high Reynolds

188   number's temperature does not significantly influence the motion because viscous

189   forces (μ) are very small when compared to inertial forces (v).

190   For turbulent flow, COMSOL Multiphysics^{TM} solves the Navier-Stokes as well

191   as continuity equations. Turbulent effects are modeled using "Turbulent Mixing"

192   interfaces for "Transport of Diluted Species" physics. In "Turbulent Mixing" models

193   the additional mixing caused by turbulence is estimated by adding turbulent diffusivity

194   to the molecular diffusivity considering:

195     $$D_T = v_T / Sc_T \qquad\qquad (3)$$

196   where D_T is the turbulent diffusion, v_T is the turbulent kinematic viscosity at 20 ^{o}C

197   (1.004E-06 m^2 s^{-1}) and Sc_T is the turbulent Schmidt number (0.7).

198   *2.4.2 Transport of dissolved and particulate components*

199   Transport of diluted and particulate components with a concentration S_i [g m^{-3}]

200   by convection and diffusion is given by:

201     $$\frac{\delta S_i}{\delta t} + (-D_T . S_i) + \mathbf{u} \cdot c_i = r_i \qquad\qquad (4)$$

202     $$r_i = \sum_j v_{j,i} * \rho_j \qquad\qquad (5)$$

203   where i = 1, 2…*m* are the different components considered (Table 2), and j is the

204   number of processes shown in Supplementary Table (4); u [m s^{-1}] is the vector of

205   velocity, r_i [g m^{-3}s^{-1}] is the reaction rate, ρ [g m^{-3}s^{-1}] is the process rate corresponding to

206   the biokinetic and chemical j processes described in Solimeno et al. (2015) [27] and $v_{j,i}$

207 is the stoichiometric coefficient. Mathematical expressions of the stoichiometric

208 coefficient and values of biokinetic, physical and chemical parameters are shown in

209 Supplementary Tables (6-9).

210 *2.4.3 Light attenuation*

211   In the present study light intensity decay was described using Lambert-Beer's

212 Law, which dictates that intensity decreases exponentially as it penetrates into a

213 perfectly homogeneous section of culture with a short penetration pathway [25], as it is

214 the case of both PBR. In this case light is attenuated by the presence of microalgae

215 inside the reactors. The average light intensity (I_{av}, [μmol m^{-2}s^{-1}]) at any point within the

216 culture is therefore calculated as [17]:

217

218 $$I_{av} = I_o \cdot \psi \, (1-\exp \, (k_i \cdot X_{ALG} \cdot d) \, / \, k_i \cdot X_{ALG} \cdot d \qquad (6)$$

219

220 where I_o [μmol m^{-2}s^{-1}] is the incident light intensity, k_i is the extinction coefficient for

221 microalgae biomass [0.1 m^2 g^{-1}] [8], X_{ALG} is the concentration of microalgae, ψ is the

222 solar irradiance fraction available in the reactor and d [m] is the diameter of tube.

223 *2.4.4 Temperature*

224   In our model, the influence of temperature on microalgae activity was

225 implemented by the thermic photosynthetic factor ($f_{T,FS}$), which takes into account the

226 effects of temperature on microalgae growth, endogenous respiration and inactivation

227 processes (1a, 1b, 2 and 3 in Supplementary Table 4, respectively). Water temperature

228 varies both on hourly and daily scales, affecting microalgal photosynthesis and

229 respiration rates. The thermic photosynthetic factor is represented in the model

230 following the work of Dauta et al. (1990) [14]:

231
$$f_{T,FS}(T) = e^{-\left(\frac{T - Topt}{s}\right)^2} \qquad (7)$$

232 where T_{opt} (optimum temperature) was assumed to be 25 °C [14] and s equal to 13 [14]

233 (it is a parameter value for empirical fitting).

2.5 Calibration procedure

235   Model output results are highly sensitive to the maximum specific growth rate of

236 microalgae (μ_{ALG}), mass transfer coefficient for oxygen ($K_{a,O2}$), and carbon dioxide

237 ($K_{a,CO2}$). The mass transfer coefficients depend on the extension of the surface interface

238 and photobioreactor design [27]. Therefore, these parameters were calibrated in the two

239 different tubular photobioreactors. The model was first calibrated using experimental

240 data obtained from the vertical photobioreactor located in Almeria (Spain). Dissolved

241 oxygen, pH, temperature and irradiance were monitored for 24 hours on February 28th,

242 2012. Afterwards, the model was calibrated with experimental data from the horizontal

243 photobioreactor located in Barcelona (Spain). Data used for this calibration were

244 retrieved from three days batch experiment from April 16th, 2012 to April 19th, 2012.

245 Available data used for the calibration procedure are shown in Supplementary Tables

246 (1-2). The initial concentrations of components in the vertical and horizontal

247 photobioreactors at the beginning of the experiments are shown in Table 3. In the

248 horizontal PBR the concentrations of NH_4^+ and NH_3 were lower than the analytical

249 method`s detection limit and therefore considered to be zero for this model. Note the

250 difference in initial concentrations of microalgae (X_{ALG}) between the two PBRs due to

251 their different operating conditions

2.6 Study cases

253   Practical study cases have been done to evaluate the influence of both

254 temperature and irradiance on microalgae production, and the effect of oxygen

255   concentration in the loop. The vertical photobioreactor of Almeria (Spain) was selected

256   as reference for these studies.

257   Starting from the initial concentrations used for calibration of the model in the

258   vertical photobioreactor, average daily microalgae production was simulated using daily

259   temperature and irradiance variations from 17th day of each month of year. Two

260   scenarios were evaluated. In the first set of simulations the vertical photobioreactor was

261   under controlled temperature by passing cooling water at 1500 L/h through an internal

262   heat exchanger located in the bubble column of the photobioreactor. In a second set of

263   simulations, temperature was obtained from meteorological annals of Almeria (Spain).

264   These two scenarios were compared and an estimation of the total annual production

265   using monthly irradiance variations was calculated. Irradiance, expressed as

266   photosynthetically active radiation (PAR), was estimated for Almeria (Spain) from the

267   mathematical equations presented in Supplementary Table 10 [2].

268   Moreover, oxygen concentration throughout the 400 m of vertical

269   photobioreactor was evaluated while maintaining the reactor under controlled

270   temperature, Dissolved oxygen profile in the loop configuration was simulated at noon

271   in the months of July and January, when the highest and lowest temperature,

272   respectively, were recorded.

273

274   **3. Results**

275   In this work simulations for two different photobioreactors were studied. First

276   we present the results of the model calibration for the vertical photobioreactor. Fig. 4

277   shows that the model was able to accurately match DO and pH trends over the course of

278   one day inside the system, with decreasing pH due to CO_2 injection (which displaces the

279   equilibrium of carbon species).

280   Fig. 5 shows the results of the calibration in the horizontal photobioreactor.

281   Experimental and simulated dissolved oxygen and pH values inside the open-air tanks

282   of the horizontal photobioreactor are presented. As can be seen, the wavelike trend of

283   pH varied due to microalgae activity, which is quite well simulated by the model.

284   Moreover, Fig. 6 shows the experimental and simulated nitrate (N_NO_3) and

285   bicarbonate (C_HCO_3) concentrations in the horizontal system. The model was able to

286   reproduce quite well the trend of experimental data. In absence of ammonia species,

287   only nitrates are used as nitrogen substrates for microalgae growth. The low

288   concentration of nitrate in the culture medium limited the activity of microalgae. As can

289   be seen, microalgae consumed nitrate concentrations quickly in the first hours of

290   experiment (Fig. 6). Likewise, Fig. 6 shows that bicarbonate concentrations decreased

291   faster in the first hours due to intense microalgae activity. After 22 hours, in absence of

292   nitrate, daily variations of bicarbonate are related to changes in equilibrium species of

293   carbon.

294   Note that, in general, simulations of the vertical PBR were more accurate than

295   those of the horizontal due to in the horizontal system there was some growth of other

296   microorganisms different from microalgae (e.g., bacteria and protozoa). This was to be

297   expected as the culture water was from an irrigation channel. The activity of these

298   microorganisms affected simulated factors though it is not known to what extent,

299   because unfortunately we do not have values for these organisms.

300   Table 4 presents the values of the parameters that were calibrated in each

301   photobioreactor. Note that maximum specific growth rate (μ_{ALG}) and the transfer of

302   gases to the atmosphere ($K_{a,O2}$ and $K_{a,CO2}$) were also calibrated in our previous works

303   [27, 28]. In this previous work the model output results are very sensitive to these

304   parameters [27, 28], and therefore should be calibrated with great accuracy.

305   Furthermore, gas transfer parameters depend on the extension of the surface interface.

306   Due to different PBRs design, modifications of these parameters were considered

307   worthwhile.

308

309   **4. Discussion**

310   *4.1 New features of the model*

311   In comparison to our previous work [27], where a 0D domain was applied, here

312   2D domain was used to represent the two tubular photobioreactors. The domain was

313   divided in two sub-domains (D1 and D2), where different conditions from the tubes

314   (D1) to the open body (D2) of the photobioreactors were applied. According to the

315   function of bubble column in the vertical system and the open-air tank in the horizontal

316   system, the transfer of gases to the atmosphere was only applied to the D2 domain that

317   corresponds to the total volume of these specific parts.

318   A periodic condition was applied at boundaries 1 and 2 to reproduce the

319   recirculation of flow from the loop configuration to the bubble column in the vertical

320   system, and from the tubes to the open-tank in the horizontal system. Simulation results

321   demonstrated that these simplifications were adequate to describe the specific parts of

322   different tubular photobioreactors. Moreover, fluid flow and transport equations were

323   added in the current model to obtain a realistic representation of the hydrodynamics in

324   the photobioreactors.

325   In addition to the previous mechanistic model presented by Solimeno et al.

326   (2015) [27] light attenuation through the medium was implemented. Light intensity

327   decays exponentially due to microalgae biomass accumulation inside the reactors.

328   Assuming a perfect mixing of medium, due to turbulent flow regime, an irradiance

329   average I_{av} was used to represent any point within the reactor.

330   *4.2 Calibration of the model*

331   Results of the sensitivity analysis, reported in our previous work [28], had

332   indicated that the maximum specific growth rate of microalgae (μ_{ALG}) and the mass

333   transfer coefficient for oxygen ($K_{a,O2}$) and carbon dioxide ($K_{a,CO2}$) were the parameters

334   with the greatest impact on simulation outputs. Therefore, calibration of these

335   parameters must occur in each particular case.

336   The calibrated maximum specific growth rate of microalgae ($\mu_{ALG} = 1.7$ [d^{-1}]) in

337   the vertical photobioreactor fits well within literature range [0.4-2.0 d^{-1}]. Also, the mass

338   transfer coefficient in the bubble column for oxygen which was $K_{a,O2} = 2.9E\text{-}03$ s^{-1} fits

339   into the range values for vertical photobioreactors [1.2E-03 to 7.7E-03 s^{-1}] [18]. The

340   mass transfer coefficient for carbon dioxide ($K_{a,CO2} = 2.8E\text{-}03$ s^{-1}) was consistent with

341   range values [1.1E-03-7.0E-03 s^{-1}] for bubble column systems [18]. These same

342   parameters were calibrated with experimental data over three days from the horizontal

343   photobioreactor located in Barcelona (Spain). Likewise as in the previous calibration,

344   the values generated for the maximum growth rate of microalgae ($\mu_{ALG} = 1.7$ [d^{-1}]), the

345   mass transfer of oxygen ($K_{a,O2} = 9.2E\text{-}03$ [s^{-1}]) and carbon dioxide ($K_{a,CO2} = 9.0E\text{-}03$ [s^{-1}]

346    $^{-1}$]) were all in agreement with literature ranges for tubular photobioreactors [9].

347   Mass transfer coefficients depend on, temperature, mixing and most importantly,

348   the extension of the surface interface. Thus, variable values of mass transfer coefficients

349   from vertical and horizontal photobioreactors are due to different design and scale-up of

350   bubble column and open-tanks, respectively.

351   Also the culture medium influences the mass transfer coefficients and the

352   maximum growth rate of microalgae. In this work the horizontal photobioreactor was

353   filled with agricultural runoff which could be contain few concentrations of bacteria and

354   other microorganisms. The activity of these microorganisms could influence dissolved

355   oxygen and carbon dioxide concentrations in the medium culture, and therefore could

356   slightly affect the values of the calibrated parameters. However, single microscopic

357   observations during the experiment indicated that their concentration was irrelevant in

358   comparison to microalgae (as usual in this type of PBR), and thus their influence is

359   considered very low or almost negligible. Calibrating the model in two different

360   photobioreactors (e.g., horizontal and vertical) with different types of media has proved

361   the robustness and resilience of the mathematical model to operate under variables

362   conditions.

363   *4.3 Study case: microalgae production as a function of temperature and irradiance*

364   Irradiance and temperature play an important role in microalgae production.

365   These physical factors influence biokinetic and chemical processes related to

366   microalgae growth. Irradiance is strictly correlated to photosynthesis rate. At high level

367   of irradiance, microalgae become 'light saturated' because photosynthesis cannot

368   process more photons. As result, the rate of photosynthesis progressively starts to

369   stabilize [9, 13]. Temperature influences the equilibrium of chemical species (carbon

370   and nitrogen), uptake of nutrients, transfer of gases to the atmosphere, and especially the

371   microalgae growth rates. The optimal temperature for microalgae growth ranges

372   between 15ºC and 25ºC, depending on the species [5, 19]. Temperature above or below

373   this range negatively affects biomass yield.

374   Thanks to the model, previously calibrated with daily experimental data, has

375   been possible to make predictions of microalgae production over long-term with

376   different environmental factors, such as temperature and irradiance. Simulations of the

377   average daily microalgae production at a monthly scale in the vertical photobioreactor

378   are presented in Fig 7. As can be observed simulations indicate that production is

379   generally higher under daily temperature variations due to a more favorable temperature

380   range (Supplementary Table 3). Table 5 presents the annual microalgae production

381   comparing the two scenarios studied: under controlled temperature and with daily

382   temperature variations. Although the growth of microalgae decreases with high

383   temperature and irradiance during the months of June, July and August (when the

384   highest temperatures of the year occur), total annual production of microalgae exposed

385   to daily temperature variations is higher than the reactor under controlled temperature.

386   To optimize production, it might be considered to only use cooling water during the

387   hottest months (June, July and August). Moreover, simulations results show that during

388   the summer the production is also inhibited due to high dissolved oxygen concentrations

389   throughout loop configuration up to 250% of air saturation (see next section).

390
391   *4.4 Study case: oxygen concentration*

392   Fig. 8 shows the simulations of the dissolved oxygen profile throughout the 400

393   m length of the vertical photobioreactor at noon (when the highest temperature occurs)

394   in the months of January and July. These two months were selected as they represent

395   the minimum and maximum microalgae activity in a monthly basis time scale. As can

396   be seen, the lower light intensity and temperature in January gives as a result lower

397   dissolved oxygen concentrations in contrast to July. Also it can be observed in both

398   months how dissolved oxygen concentration increases throughout the loop and

399   decreases in the bubble column. In July, transfer of excess of dissolved oxygen to the

400   atmosphere throughout the airlift permits to re-establish, at the beginning of loop

401   configuration, the oxygen level under the maximum concentration of oxygen dissolved

402   in water ($32 \ gO_2 \ m^{-3}$) equal 350% of saturation ($9.07 \ gO_2 \ m^{-3}$) [1, 8]. This property of

403   the photobioreactor design is especially important in warm months (such as July), when

404   a high photosynthetic activity could cause inhibition due to oxygen accumulation.

405   The model presented in this work allows to simulate and study microalgae

406   growth inhibition due to high dissolved oxygen concentrations thanks to the inclusion of

407   a photorespiration factor $f_{PR}(S_{O2})$ [27]. The function ($f_{PR}(S_{O2})$) in Fig. 9 describes that

408   for dissolved oxygen concentrations lower than the $250\% S_{O2}^{SAT}$ ($22.67 \ gO_2 \ m^{-3}$) the

409   photosynthesis rate is reduced by 10%. Above this value, the photosynthesis rate

410   decrease more quickly with a vertical asymptote and is equal at zero when dissolved

411   oxygen reaches the 350% saturation limit (τS_{O2}^{SAT} = 32 gO_2 m^{-3}).

412   In process design, the current model can be used to find the maximum

413   photobioreactor length to avoid oxygen inhibition. For example, for the month of July,

414   simulations were conducted using half the previous bubble column volume (from 0.44

415   m^3 to 0.22 m^3) in the vertical photobioreactors loops (400 m and 250 m). As seen in Fig.

416   10, reducing the volume of the bubble column and keeping the original loop

417   configuration length (400 m), the simulation results show that the DO exceeds the

418   saturation limit l inhibiting microalgae growth. The volume of bubble column is not

419   enough to transfer the excess of dissolved oxygen to the atmosphere. On the contrary,

420   simulations indicate that a 250 m length, photobioreactor greatly reduces the oxygen

421   accumulation.

422

423   **5. Conclusion**

424   In this paper a new mechanistic model to simulate microalgae growth was

425   calibrated in two different tubular photobioreactors. Fluid flow, transport equations and

426   light attenuation were included in the model described in our previous work and

427   implemented in COMSOL Multiphysics^{TM} software. Uncertainty parameters from

428   previous sensitivity analysis were calibrated in each photobioreactor. The results of

429   calibration indicate that the mass transfer of gases and the maximum specific growth

430   rate of microalgae fit well within literature ranges. Moreover, the developed model

431   demonstrates potential prediction of oxygen accumulation throughout the loop

432   configuration and daily microalgae production as a function of temperature and

433   irradiance. The model proves to be an efficient tool for photobioreactor design and

434   production optimization.

435

436   **References**

437   [1] Acién Fernández F.G., Fernández Sevilla, J.M., Molina Grima, E. 2013. Photobioreactors

438   for the production of microalgae. Reviews in Environmental Science and Bio/Technology,

439   Volume 12, Issue 2, pp 131-151.

440   [2] Al-Rawahi, N.Z., Zurigat, Y.H., Al-Azri N.A. 2011. Prediction of Hourly Solar Radiation on

441   Horizontal and Inclined Surfaces for Muscat/Oma. The Journal of Engineering Research, Vol 8,

442   No 2, 19-31.

443

444   [3] APHA-AWWA-WPCF, 2001. APHA-AWWA-WPCF Standard Methods for the

445   Examination of Water and Wastewater, twentieth ed. American Public Health association,

446   Washington DC.

447

448   [4] Bernard, O., Masci, P., Sciandra, A., 2009. A photobioreactor model in nitrogen limited

449   conditions. In: Proceedings of the sixth conference on mathematical model- ling, Vienna.

450   [5] Bitog, J.P., Lee, I.-B., Lee, C.-G., Kim, K.-S., Hwang, H.-S., Hong, S.-W., Seo, I.-H.,

451   Kwon, K.-S., Mostafa, E. 2011. Application of computational fluid dynamics for modelling and

452   designing photobioreactors for microalgae production: A review. Computers and Electronics in

453   Agriculture, 76(2), 131–147.

454   [6]. Bonachela, J.A., Raghib, M., Levin, S.A. 2011. Dynamic model of flexibile phytoplankton

455   nutrient uptake. Proc. Natl. Acad. Sci. U.S.A. 108, 20633-200638.

456   [7] Boussiba, S. Shadler, T., Karamanos, T.Y., Mollion, J., Morva, H., Verdus, M.C.,

457   Christiaen, D. 1986 Anabaena azollae as a nitrogen biofertilizer. Algal biotechnology, 169-178.

458   [8] Camacho Rubio F., García Camacho F., Fernández Sevilla J.M., Chisti Y., Molina Grima E.,

459   2003. A mechanistic model of photosynthesis in microalgae. Biotechnol Bioeng. 81(4): 459–73.

460   [9] Camacho Rubio F., Acién Fernández F.G., García Camacho F., Sánchez Pérez J.A., Molina

461   Grima E., 1999. Prediction of dissolved oxygen and carbon dioxide concentration profiles in

462   tubular photo- bioreactors for microalgal culture. Biotechnology and bioengineering 62, 71–86.

463 [10] Carvalho, L. B., Souza, M. C., Bianco, M. S., Bianco, S. 2011. Estimativa da área foliar de

464 plantas daninhas de ambiente aquático: Pistia stratiotes. Planta daninha, v. 29, n. 1, p. 65-68,

465 2011.

466 [11] Chisti, Y., 2007. Biodiesel from microalgae. Biotechnology Advances 25, 294‑306.

467 [12] Costache T. A, Acién Fernández F.G., Morales M., Fernández Sevilla J.M., Stamatin, I.,

468 Molina, E., 2013 Comprehensive model of microalgae photosynthesis rate. Appl Microbiol

469 Biotechnol., 17:7627-37

470 [13] Craggs, R.J., Heubeck, S., Lundquist, T.J., Benemann, J.R. 2011. Algae biofuel from

471 wastewater treatment high rate algal ponds. Water Sci. Technol. 63(4), 660-665.

472 [14] Dauta, A., Devaux, J., Piquemal, F., Boumnich, L. 1990. Growth rate of four freshwater

473 algae in relation to light and temperatura. Hydrobiologia 207, 221-226.

474 [15] Fernández, I. Acién, F.G., Berenguel, M., Guzmán J.L., Andrade, G.A., Pagano, D.J. 2014.

475 A Lumped parameter chemical-physical model for tubular photobioreactors. Chemical

476 Engineering Science 112, 116-129.

477 [16] Fernández, I., Acién, F.G., Fernández, J.M., Guzmán, J.L., Magán, J.J., Berenguel, M.

478 2012. Dynamic model of microalgal production in tubular photobioreactor. Biosource

479 Technology 126, 172-181.

480 [17] Hase, R., Oikawa, H., Sasao, C., Morita, M., Watanabe, Y., 2000. Photosynthetic

481 production of microalgal biomass in a raceway system under greenhouse conditions in Sendai

482 city. J. Biosci. Bioeng. 89 (2), 157–163.

483 [18] Hulatt, C.J., Thomas, D.N., 2011. Productivity, carbon dioxide uptake and net energy

484 return of microalgal bubble column photobioreactors. Biosour. Technol. 102, 5775-5787.

485 [19] Larsdotter, K., 2006. Wastewater treatment with microalgae-a literature review. Vatten,

486 31–38.

487   [20] Molina Grima, E., Fernández, J., Acién Fernández, G., Chisti, Y., 2001. Tubular

488   photobioreactor design for algae cultures. Journal of biotechnology 92, 113–131.

489   [21] Molina Grima, E., 1999. Mass culture methods. In: Flickinger, M.C., Drew, S.W. (Eds.),

490   Encyclopedia of Bioprocess Technology: Fermentation, Biocatalysis and Bioseparation, vol. 3.

491   Wiley, pp. 1753–1769.

492   [22] Novak, J.T., Brune, D.E. 1985. Inorganic carbon limited growth kinetics of some

493   freshwater algae. Water Res. 19, 215-225.

494   [23] Packer A, Li Y, Andersen T, Hu Q, Kuang Y, Sommerfeld M. 2011. Growth and neutral

495   lipid synthesis in green microalgae: a mathematical model. Bioresour Technol; 102:111–7.

496   [24] Reichert, P., Borchardt, D., Henze, M., Rauch, W., Shanahan, P., Somlyódy, L.,

497   Vanrolleghem, P., 2001. River Water Quality Model no. 1 (RWQM1): II. Biochemical process

498   equations. Water science and technology : a journal of the International Association on Water

499   Pollution Research 43(5), 11–30.

500   [25] Sanchez, J.F., Fernández-Sevilla, J.M., Acíen, F.G., Ceron, M.C., Perez-Parra, J. &

501   Molina-Grima, E., 2008. Biomass and lutein productivity of Scenedesmus almeriensis:

502   influence of irradiance, dilution rate and temperature. Appl. Microbiol. Biotechnol., 79, 719–

503   729.

504   [26] Silva, H.J., Pirt, J. 1984. Carbon dioxide inhibition of photosynthetic growth of chlorella.

505   Journal of General Microbiology, 130, 2833-2838.

506   [27] Solimeno, A., Samsó, R., Uggetti, E., Sialve, B., Steyer, J.P., Gabarró, A., García, J. 2015.

507   New mechanistic model to simulate microalgae growth. Algal Research 12, 350-358.

508   [28] Solimeno. A., Samsó, R., García, J. 2016. Parameter sensitivity analysis of a mechanistic

509   model to simulate microalgae growth. Algal Research 15, 217-223.

510   [29] Stokes, G. 1851. On the Effect of the Internal Friction of Fluids on the Motion of

511   Pendulums. Transactions of the Cambridge Philosophical Society 9: 8–106.

512   [30] Ugwu, C.U., H. Aoyagi and H. Uchiyama, 2008. Photobioreactors for mass cultivation of

513   algae. Bioresour. Technol., 99: 4021-4028.

514   [31] Wang, B., Lan, Q., Horsman, M., 2012. Closed photobioreactors for production of

515   microalgal biomasses. Biotechnology Advances 30 904–912.

516   [32] Weissmand, J.C., Goebel, R.P., 1987. Design and Analysis of Microalgal Open Pond

517   Systems for the Purpose of Producing Fuels. SERI/STR-231-2840.

518   [33] Wu, X., Merchuk, J., 2001. A model integrating fluid dynamics in photosynthesis and

519   photoinhibition processes. Chemical Engineering Science 56, 3527–3538.